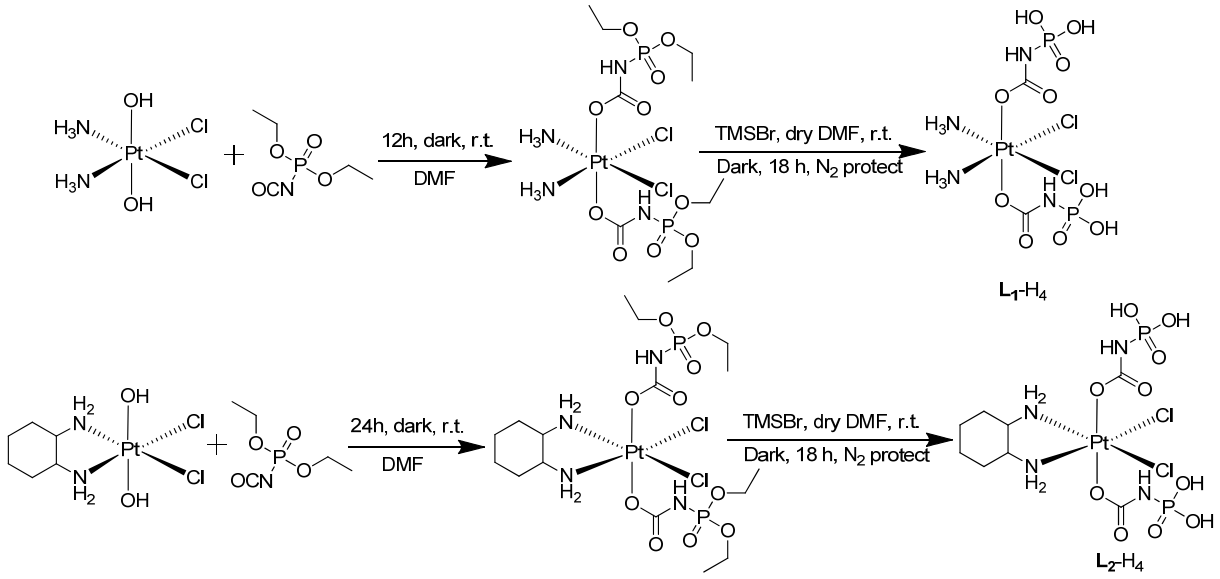

Supplementary Figure 1. Synthesis of bisphosphonic acid ligands based on Pt(IV) prodrugs.

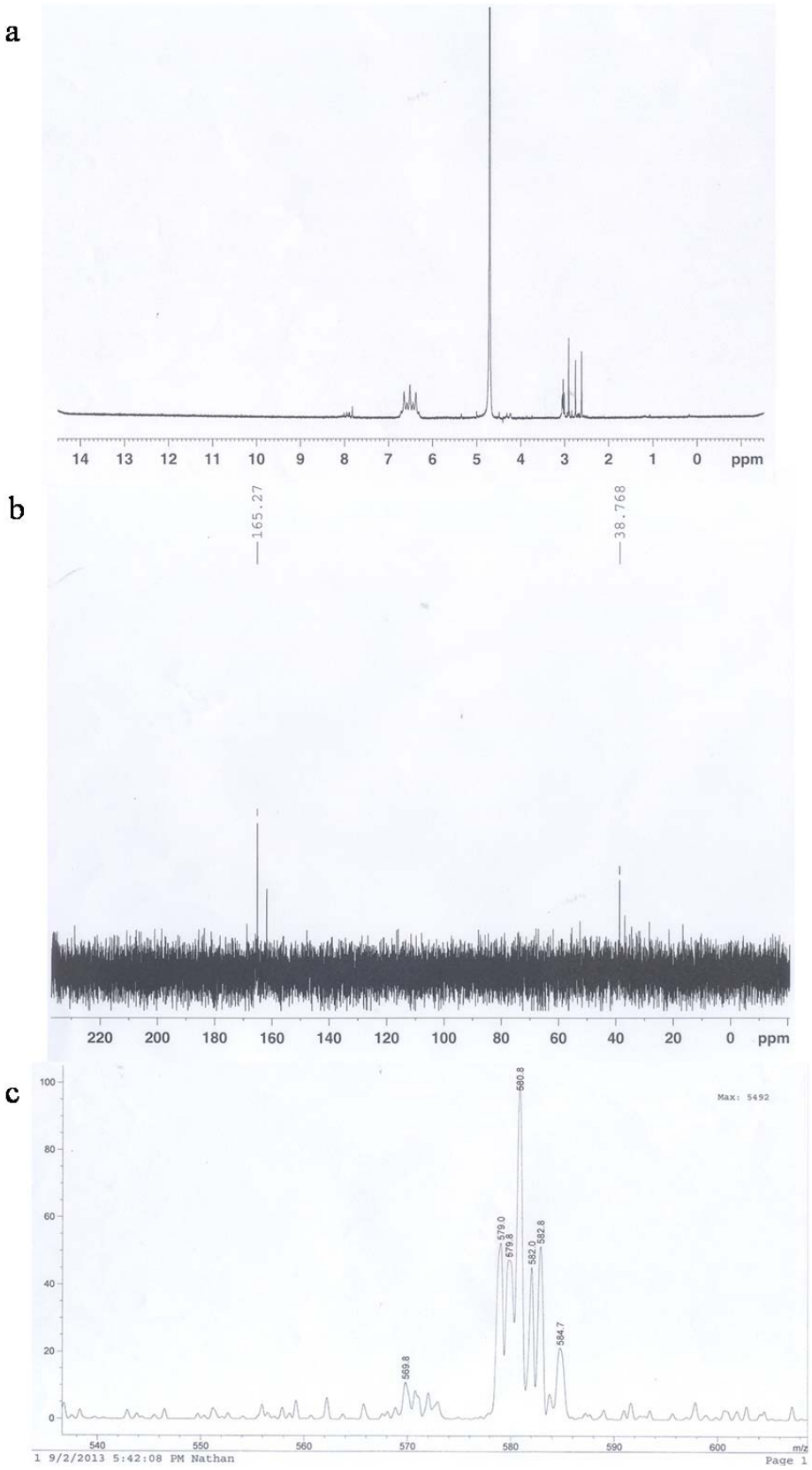

Supplementary Figure 2. ^{1}H NMR (a), ^{13}C NMR (b), and mass spectrum (c) of $\mathbf{L_1}$-H_4.

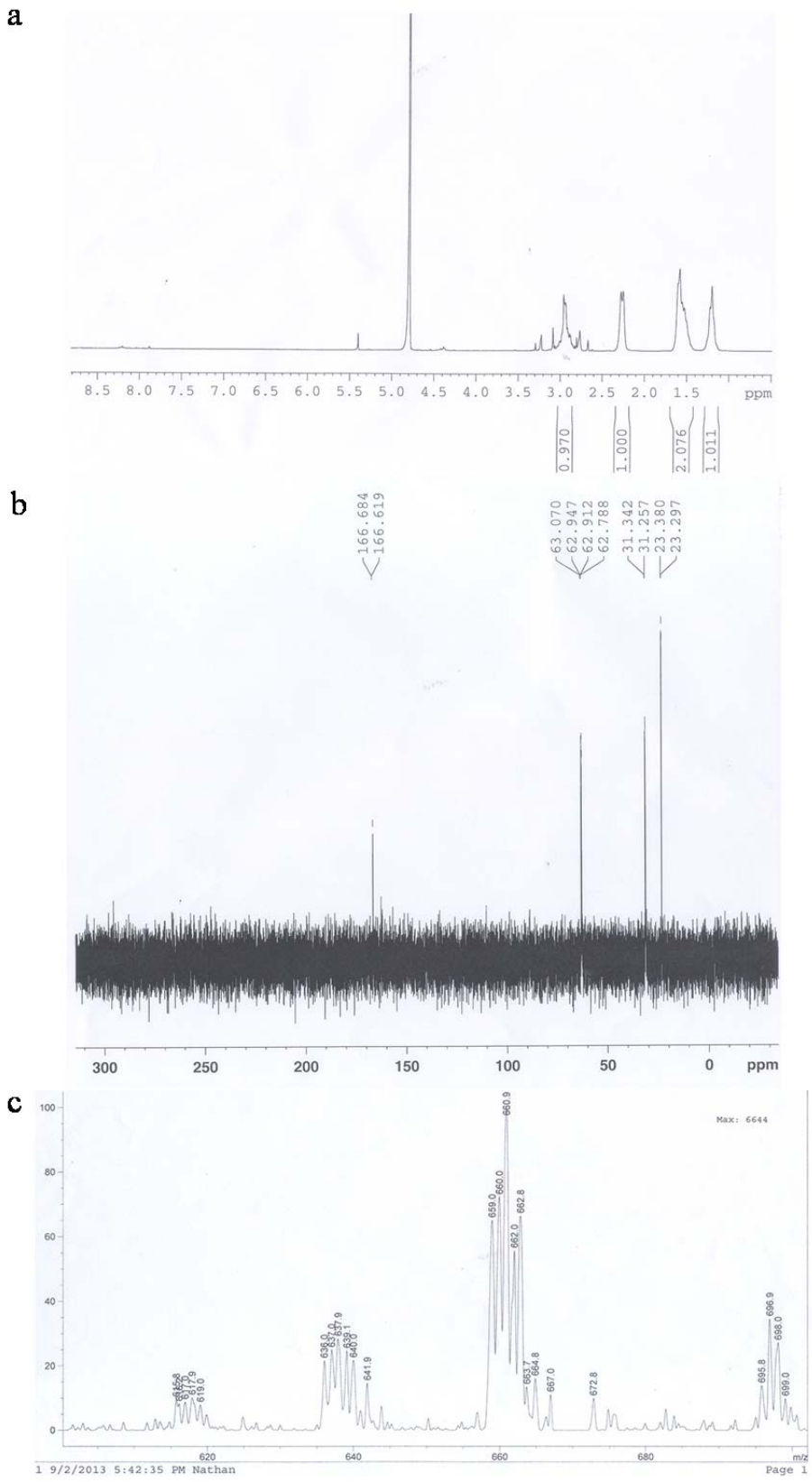

Supplementary Figure 3. ^{1}H NMR (a), ^{13}C NMR (b), and mass spectrum (c) of $\mathbf{L_2}$-H_4.

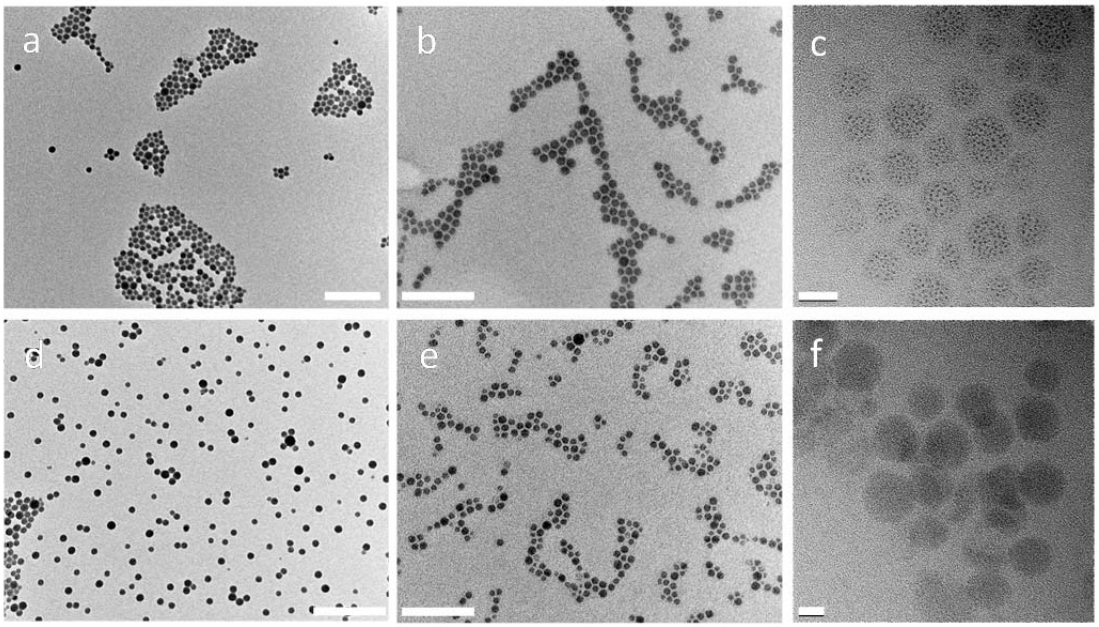

Supplementary Figure 4. Low resolution TEM images of a) **1**, b) **1P**, d) **2**, and e) **2P**. Scale bars = 200 nm. High resolution TEM images of c) **1P** and f) **2P**. Scale bars = 20 nm. The cisplatin prodrugs in NCP particles appeared to have been reduced by the electron beams during high resolution TEM imaging.

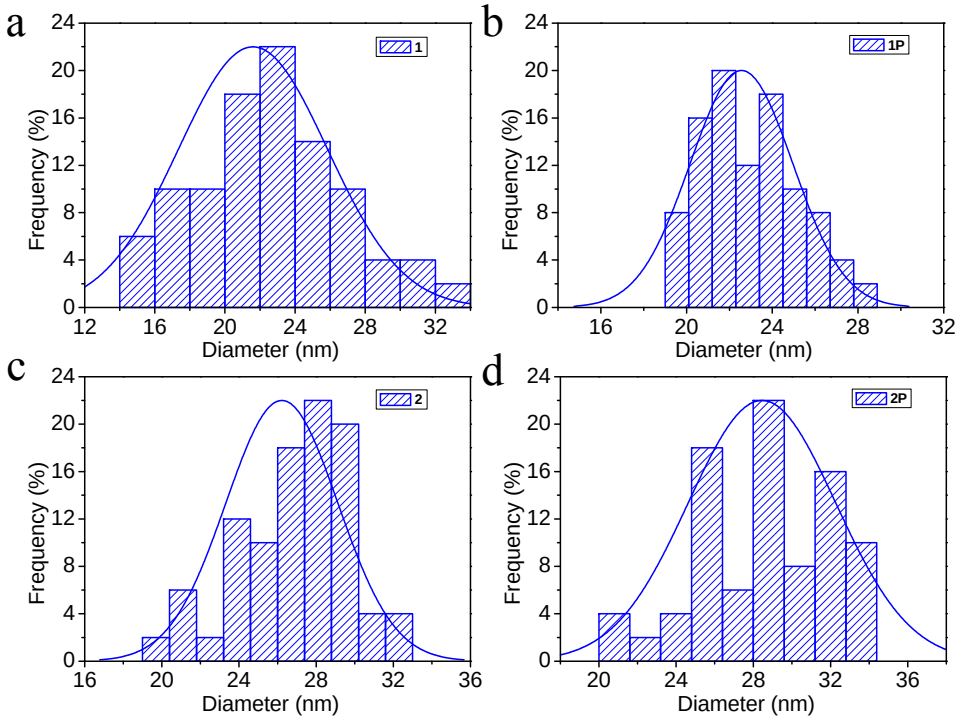

Supplementary Figure 5. Size distribution obtained from TEM images of a) **1**, b) **1P**, c) **2**, and d) **2P**.

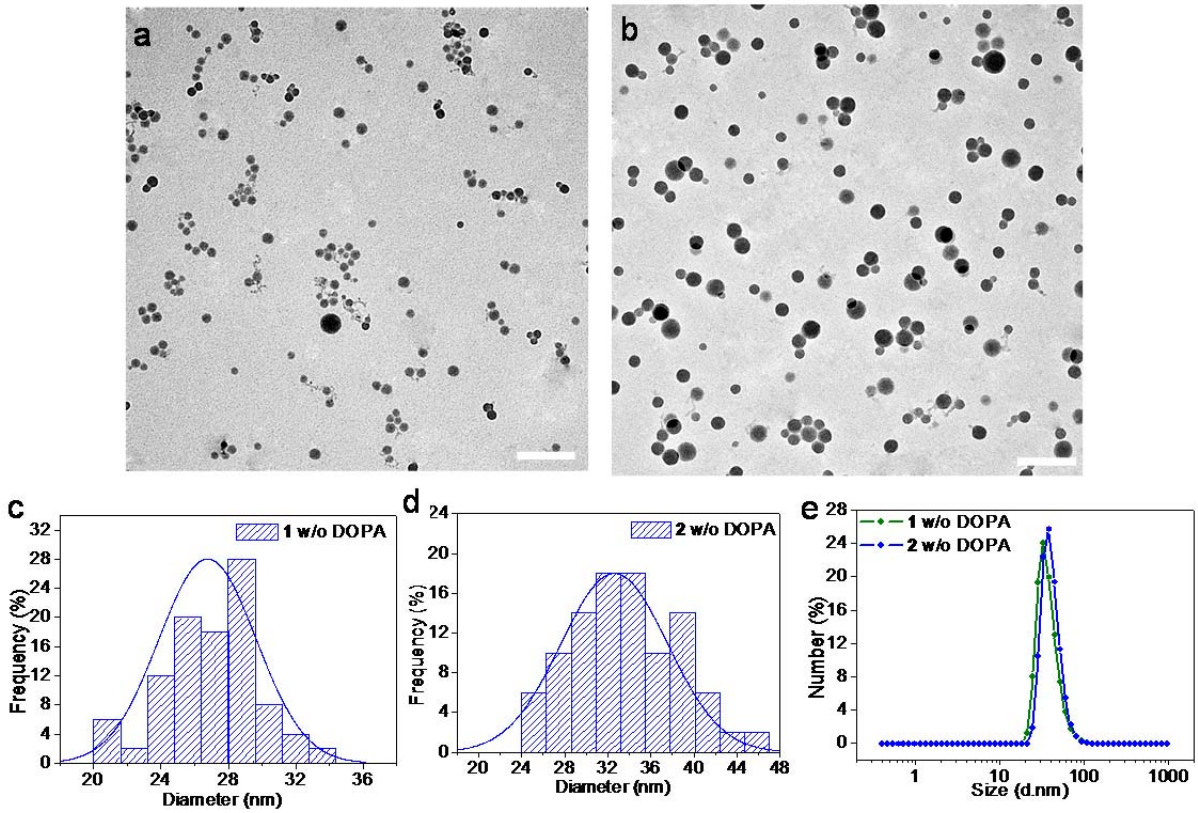

Supplementary Figure 6. TEM images of a) DOPA free **1**, b) DOPA free **2**. Size distribution obtained from TEM images of c) DOPA free **1**, and d) DOPA free **2**. e) Size distribution measured by DLS. Scale bars = 200 nm.

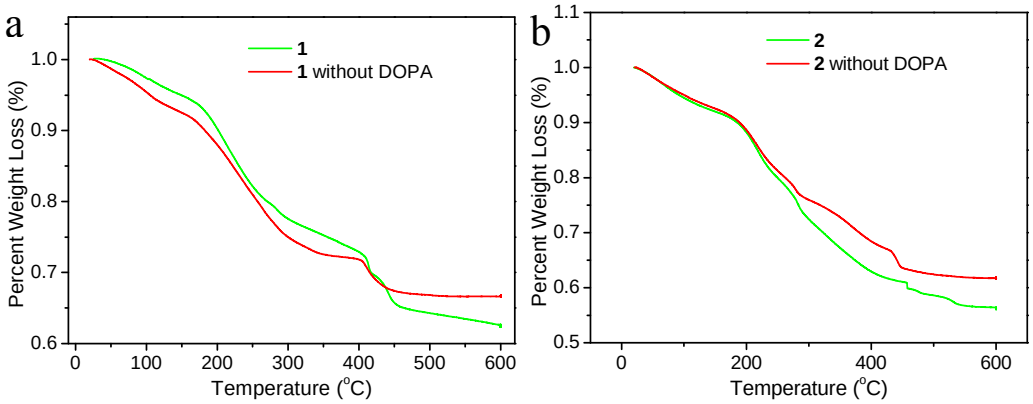

Supplementary Figure 7. Thermogravimetric analysis (TGA) curves of **1** (a) and **2** (b).

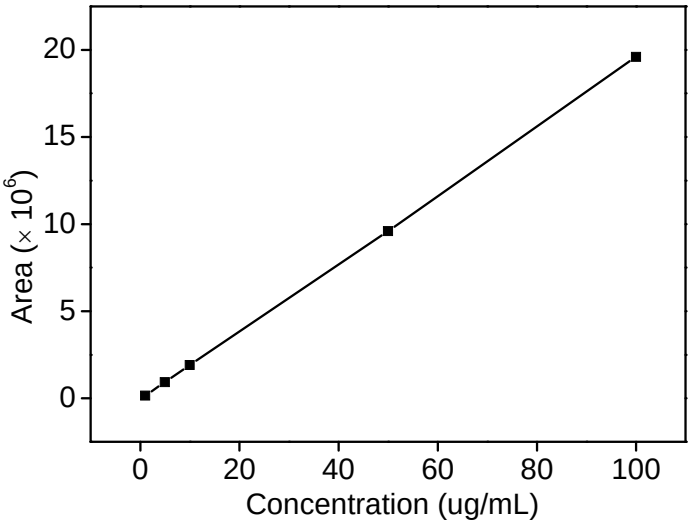

Supplementary Figure 8. The standard curve of Triton X-100 constructed from HPLC measurements.

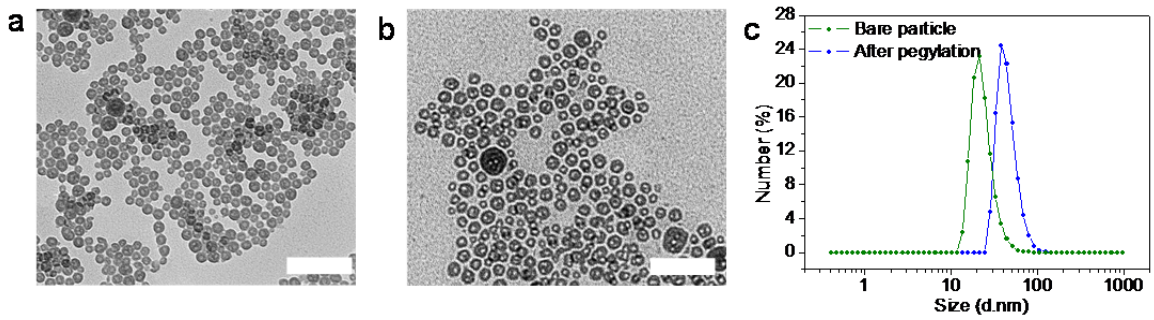

Supplementary Figure 9. TEM images of a) bare and b) pegylated Zn Control. c) Size distribution of Zn Control particles measured by dynamic light scattering. Scale bars= 100 nm.

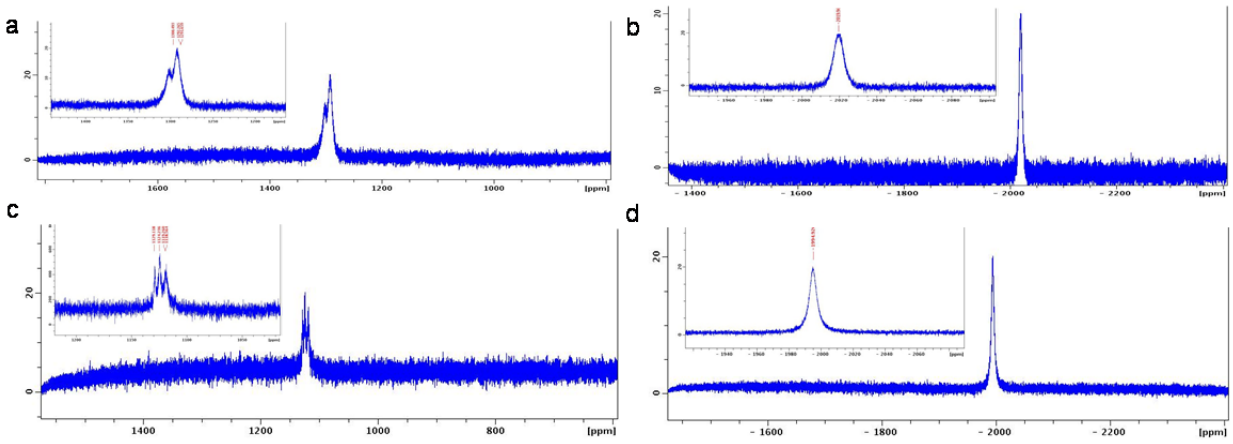

Supplementary Figure 10. The ^{195}Pt NMR spectra of $\mathbf{L_1}$-H_4 (a) and $\mathbf{L_2}$-H_4 (c) before reduction. The ^{195}Pt NMR spectra of $\mathbf{L_1}$-H_4 (b) and $\mathbf{L_2}$-H_4 (d) after reduction by cysteine.

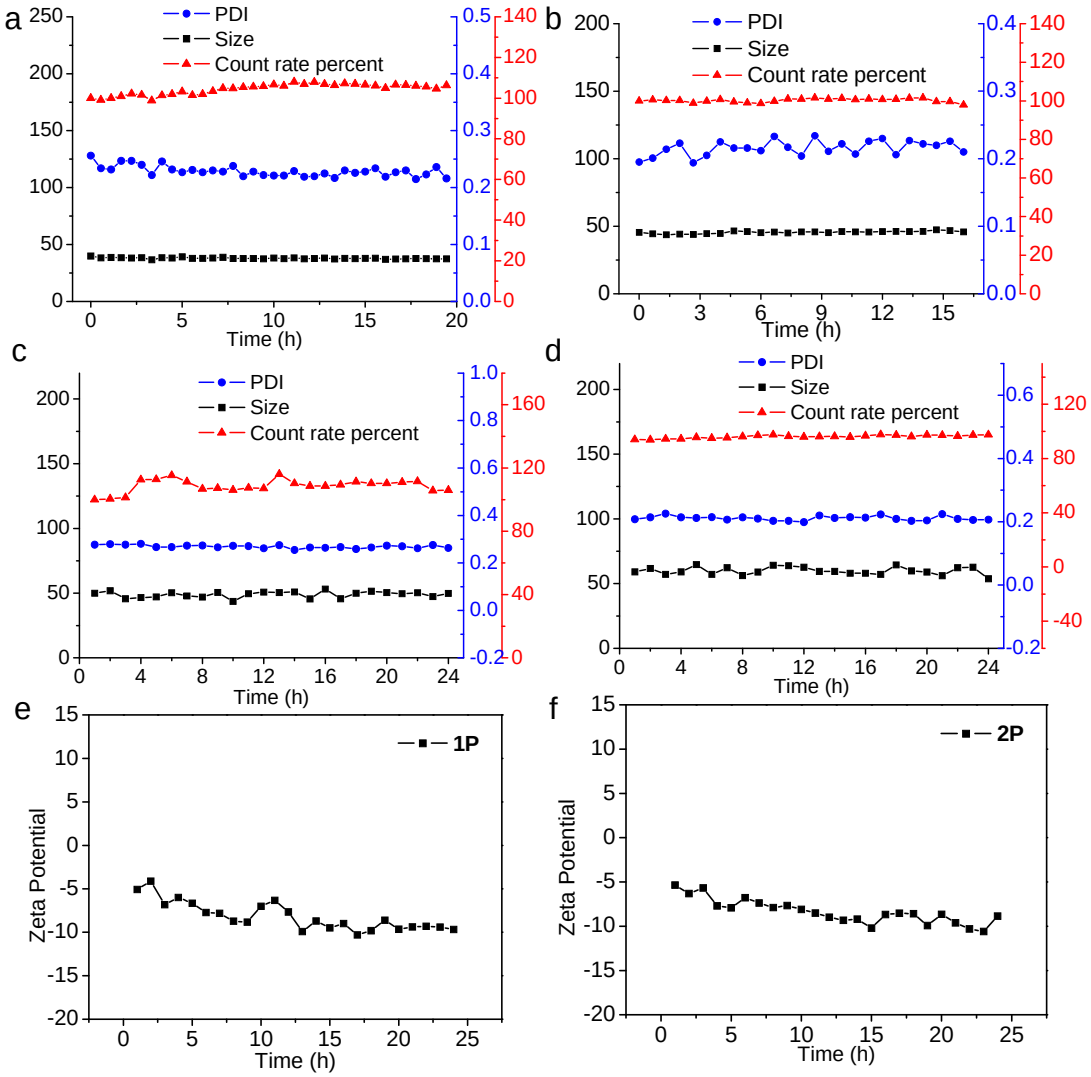

Supplementary Figure 11. Stability test of **1P** (a) and **2P** (b) in PBS buffer with BSA at 37 °C. Stability test of **1P** (c) and **2P** (d) in PBS with 10% FBS at 37 °C. Zeta potential measurements of **1P** (e) and **2P** (f) in PBS with 10% FBS at 37 °C.

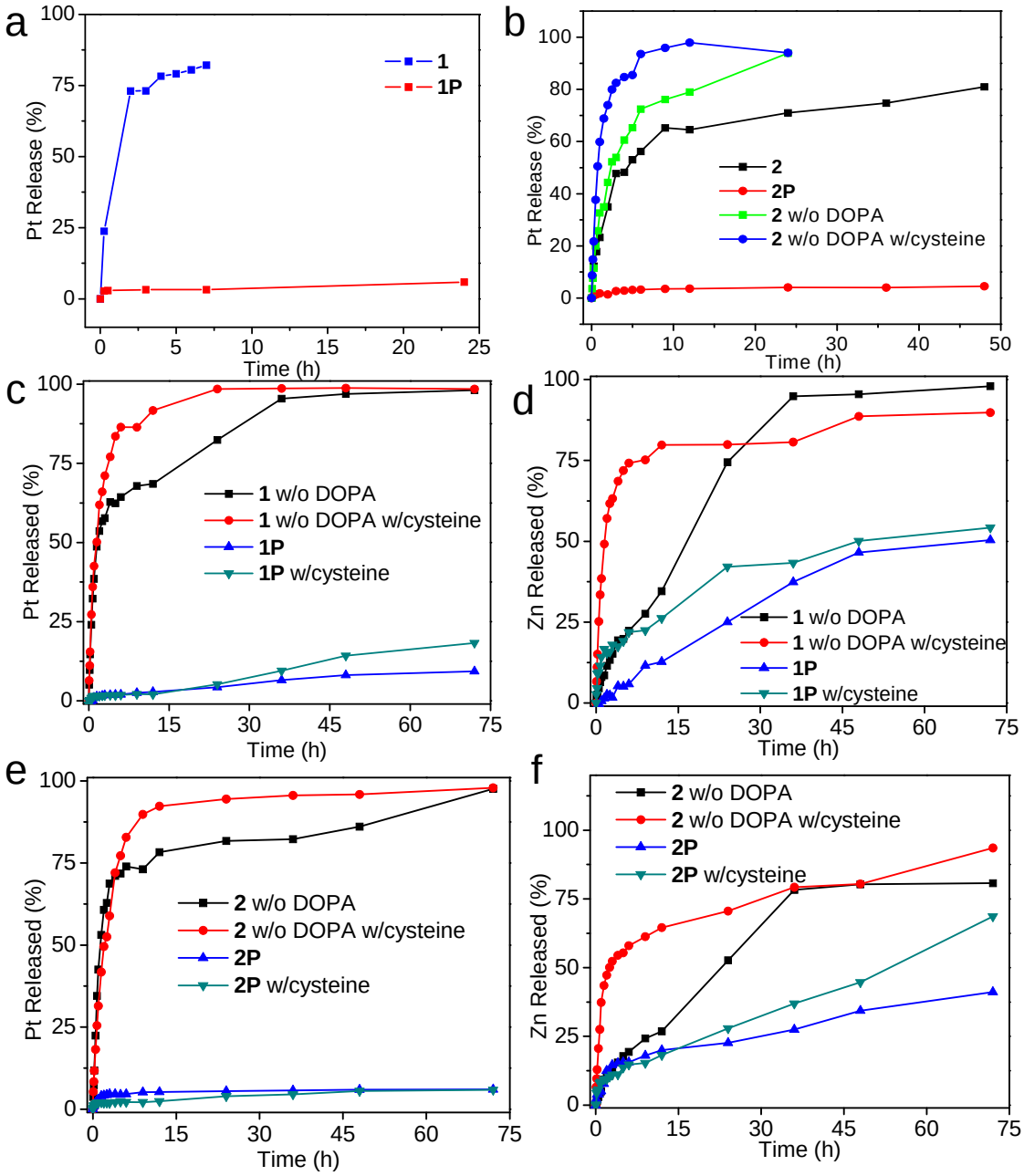

Supplementary Figure 12. Release profiles of **1**, **1P** (a), **2**, and **2P** (b) in 5mM PBS at 37 °C. Release profiles of Pt (c) and Zn (d) for **1**, and Pt (e) and Zn (f) for **2** in cell culture medium supplemented with 10% FBS at 37 °C.

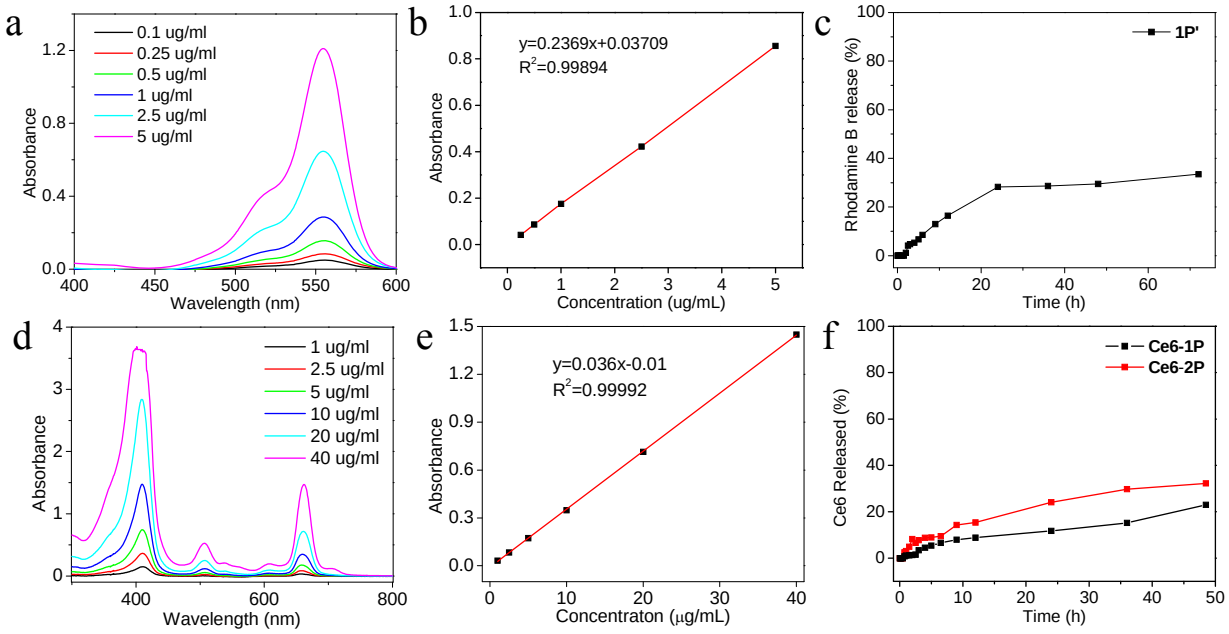

Supplementary Figure 13. a) Absorption spectra of rhodamine B in cell culture medium supplemented with 10% FBS (background subtracted). b) Calibration curve of UV-Vis absorption of rhodamine B in cell culture medium supplemented with 10% FBS. c) Release profile of rhodamine B from **1P'** in cell culture medium supplemented with 10% FBS at 37 ^{o}C, monitored by UV-Vis spectroscopy. d) Absorption spectra of chlorin e6 (Ce6) in cell culture medium supplemented with 10% FBS (background subtracted). e) Calibration curve of UV-Vis absorption of Ce6 in cell culture medium supplemented with 10% FBS. f) Release profile of Ce6 from Ce6-**1P** and Ce6-**2P** in cell culture medium supplemented with 10% FBS at 37 ^{o}C, monitored by UV-Vis spectroscopy.

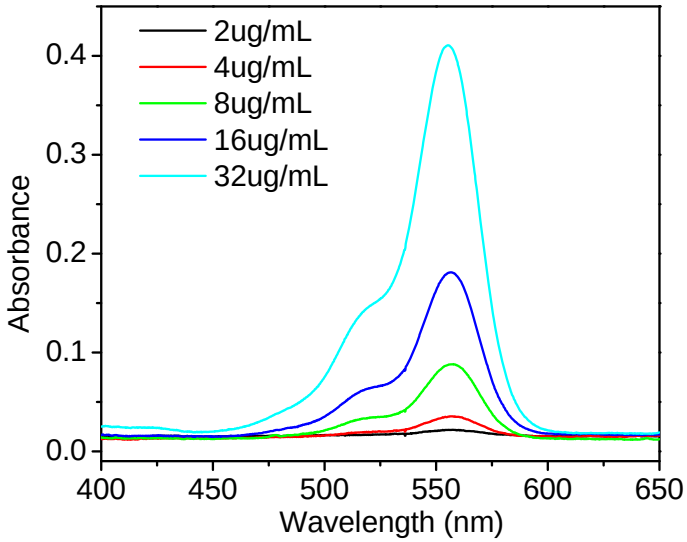

Supplementary Figure 14. UV-Vis absorption spectra of rhodamine B in THF.

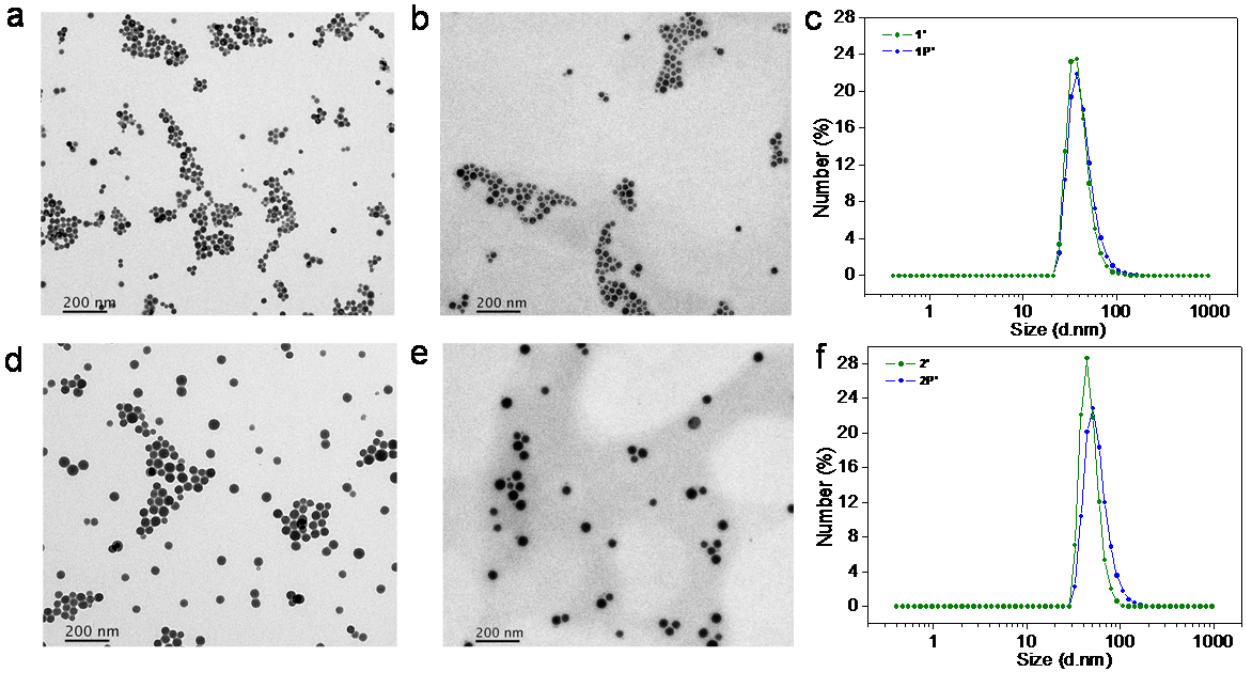

Supplementary Figure 15. TEM images of a) **1'**. b) **1P'**. d) **2'**. e) **2P'**. Size distribution of **1'** (c) and **2'** (f) measured by dynamic light scattering.

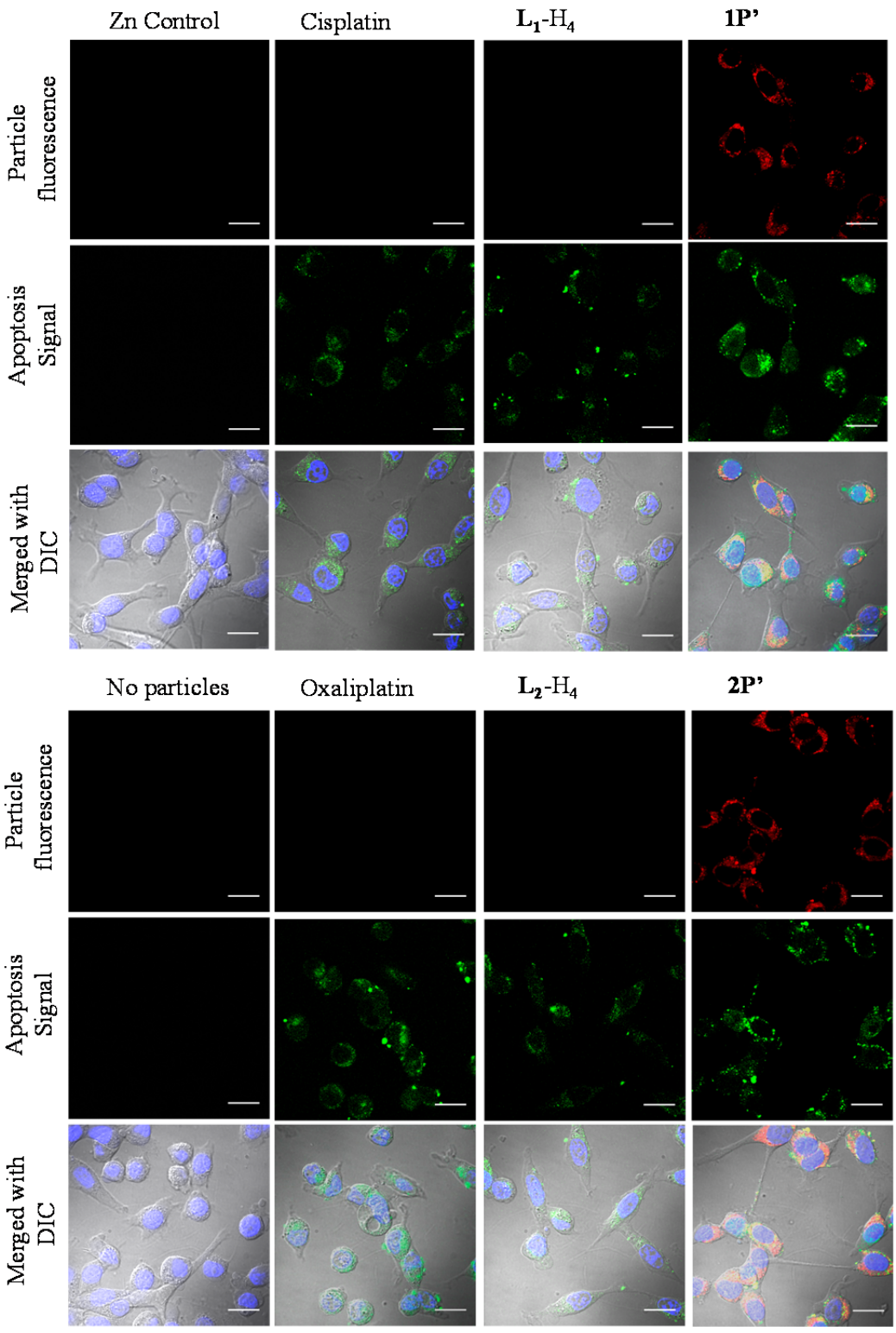

Supplementary Figure 16. Fluorescence images of CT26 cells incubated with various formulations. Channels are: apoptosis by TUNEL assays (green), and rhodamine B doped NCPs (Red). Scale bars are 20 μm.

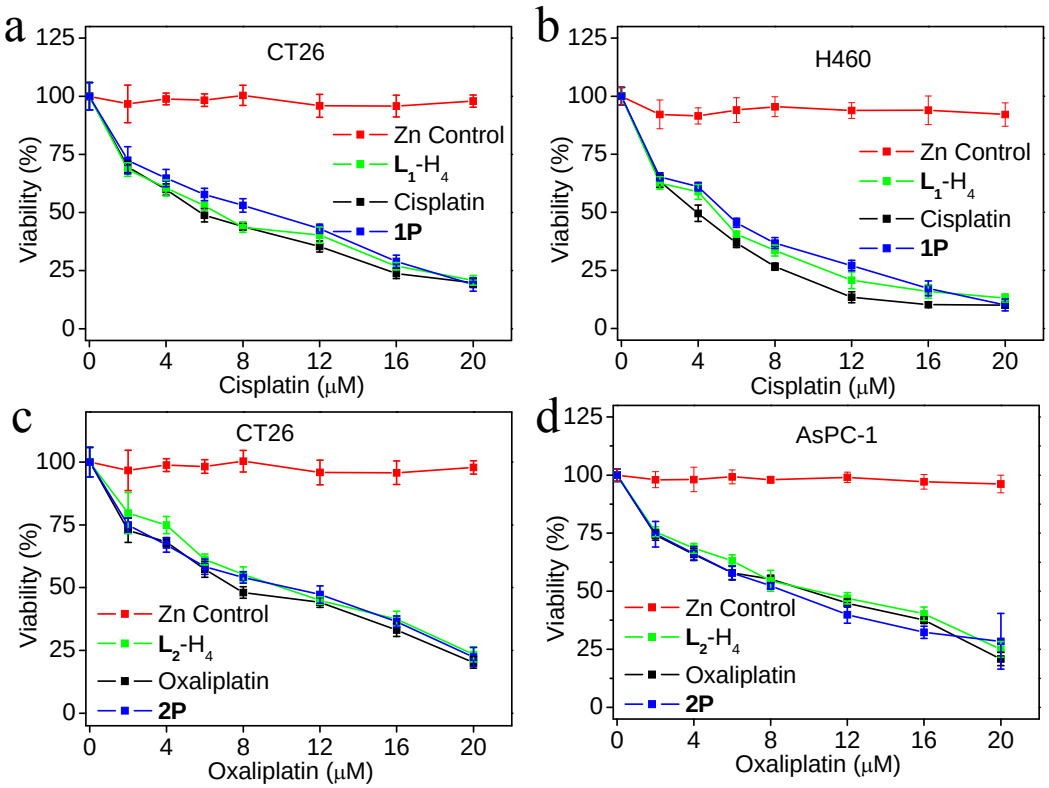

Supplementary Figure 17. Cytotoxicity assay of Zn Control, cisplatin, $\mathbf{L_1}$-H_4, and **1P** against CT26 (a) and H460 (b) cell lines. Cytotoxicity assay of Zn Control, oxaliplatin, $\mathbf{L_2}$-H_4, and **2P** against CT26 (c) and AsPC-1 (b) cell lines.

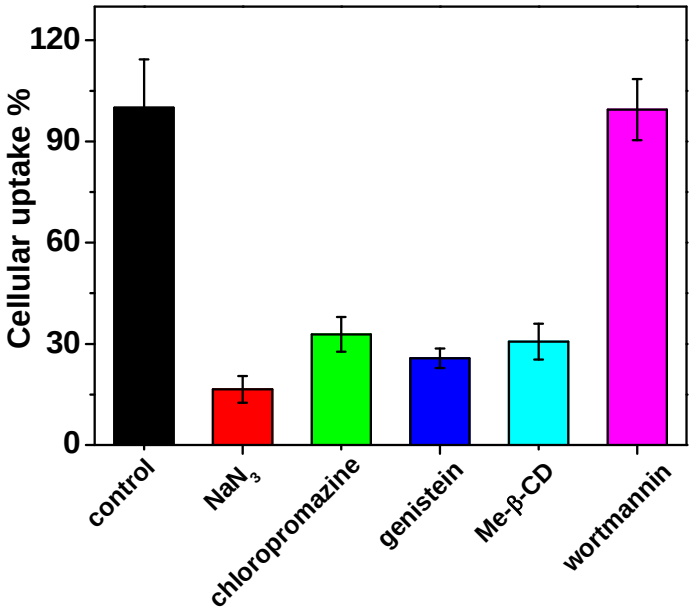

Supplementary Figure 18. The Pt uptake amount in CT26 cells after pre-incubation with various inhibitors as determined by ICP-MS. Data are expressed as means±SD.

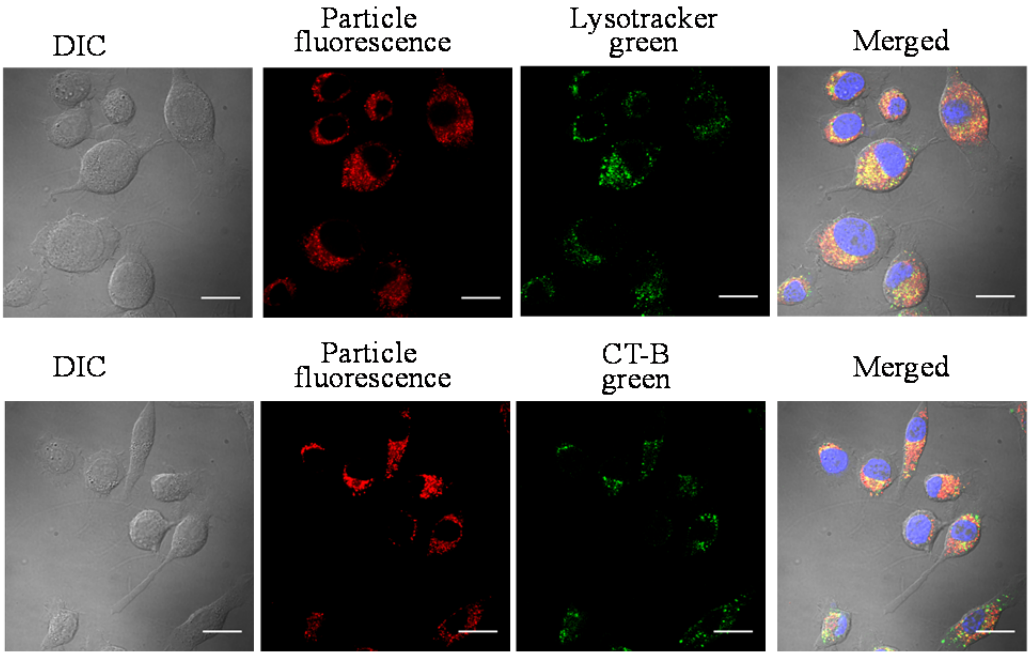

Supplementary Figure 19. Fluorescence images of CT26 cells incubated with **1P'**. Channels are: rhodamine B doped NCPs (Red) and Lysoracker green or Chlorea Toxin Subunit B (green). Scale bars are 20 μm.

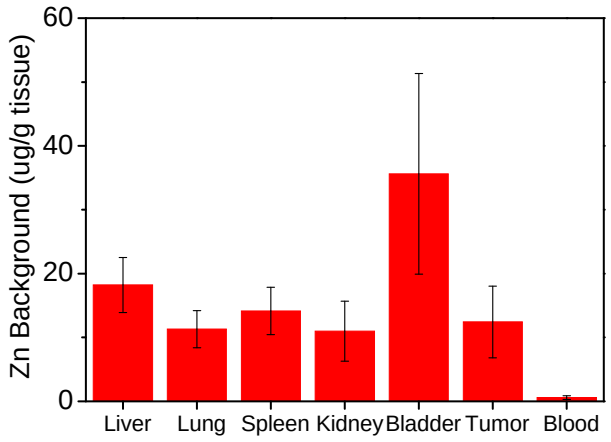

Supplementary Figure 20. Zn background concentrations in mouse organs. Data are expressed as means±SD (n=3).

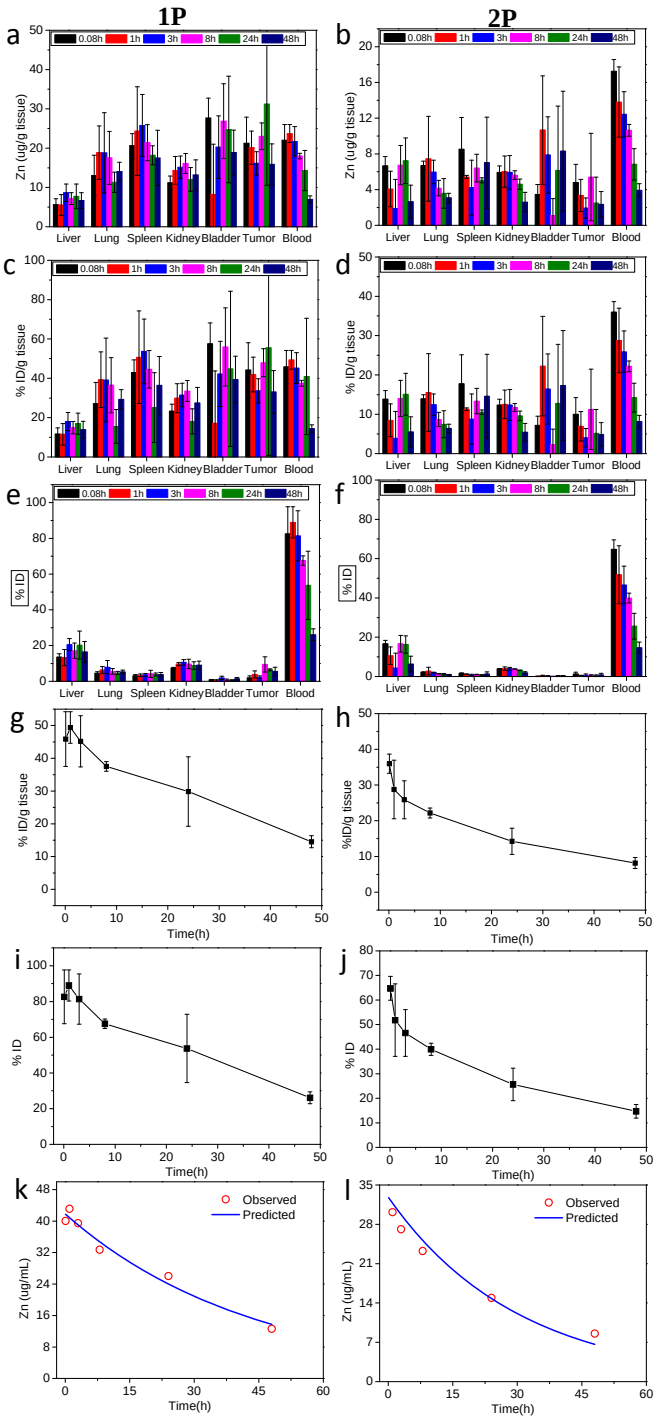

Supplementary Figure 21. Tissue distribution and blood circulation profiles assessed by Zn for **1P** (a, c, e, and g), and **2P** (b, d, f, and h). Data are expressed as means±SD (n=3). Observed and fitted time-dependent Zn concentrations in plasma following **1P** (k) and **2P** (l) administration.

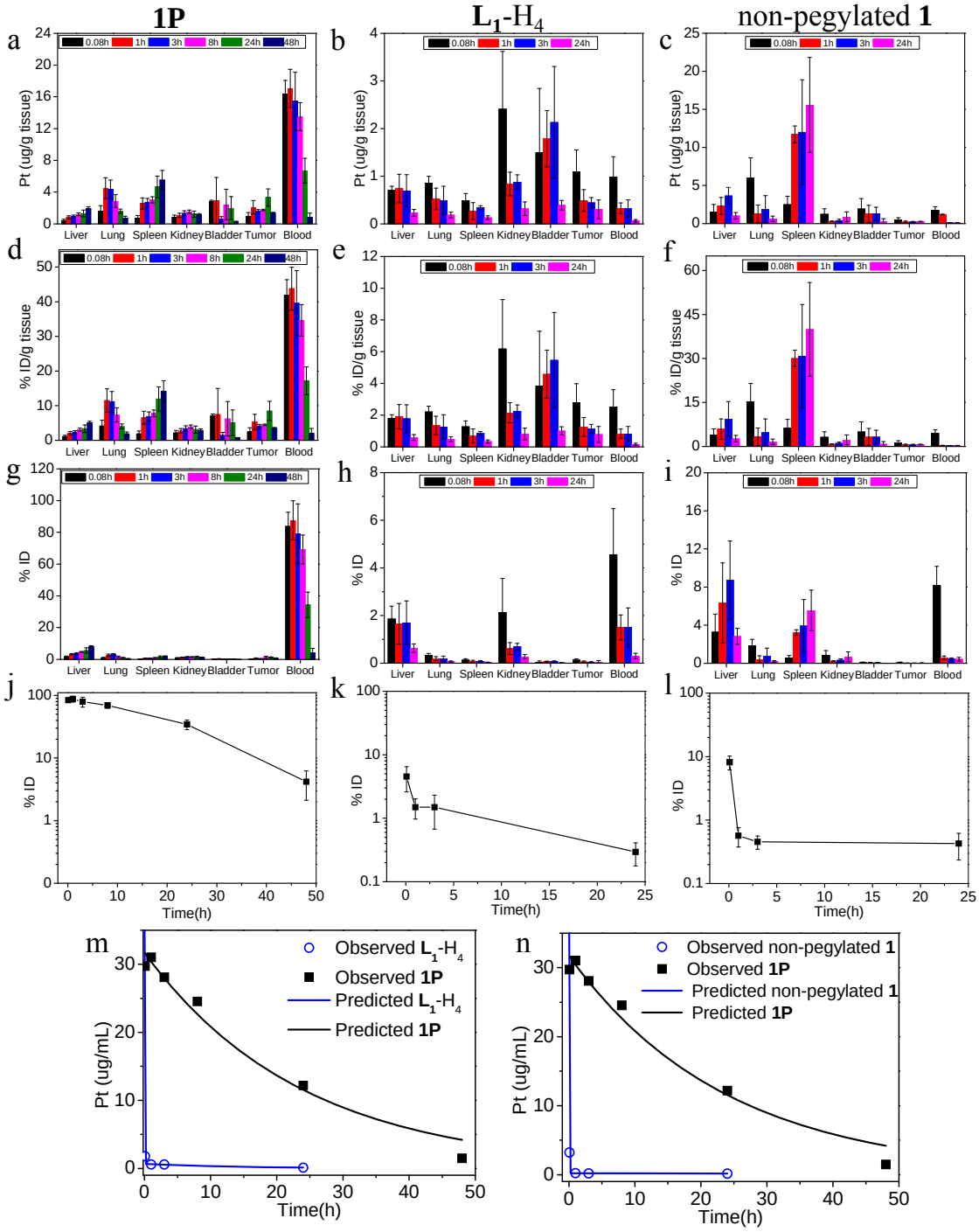

Supplementary Figure 22. Tissue distribution and blood circulation profiles of **1P** (a, d, g, and j), **L$_1$**-H$_4$ (b, e, h, and k), and non-pegylated **1** (c, f, i, and l). Data are expressed as means±SD (n=3). Observed and fitted time-dependent Pt concentrations in plasma following **1P**, **L$_1$**-H$_4$ (m) and non-pegylated **1** (n) administration.

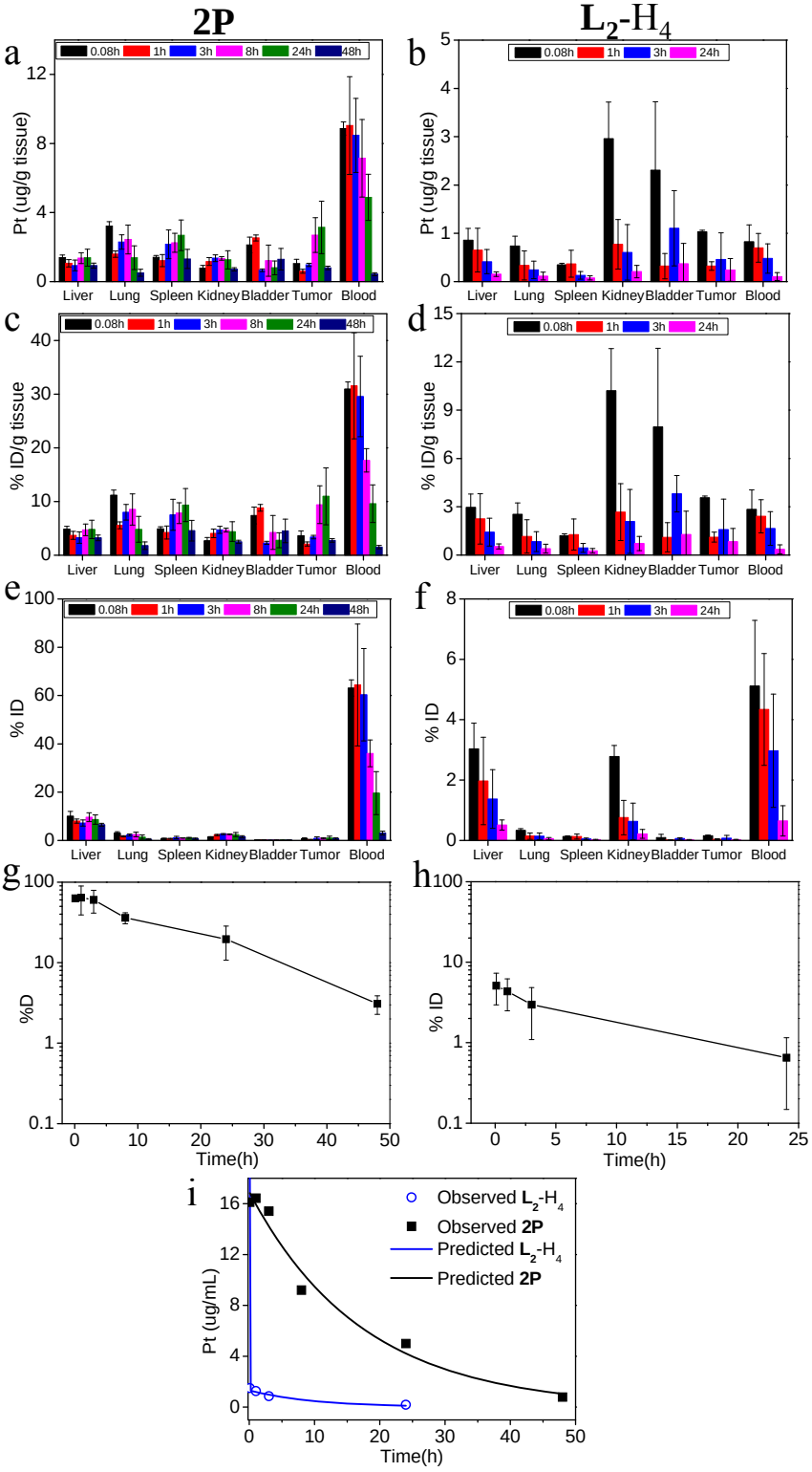

Supplementary Figure 23. Tissue distribution and blood circulation profiles of **2P** (a, c, e, and g) and **L**$_2$-H$_4$ (b, d, f, and h. Data are expressed as means±SD (n=3). Observed and fitted time-dependent Pt concentrations in plasma following **2P** and **L**$_2$-H$_4$ administration (i).

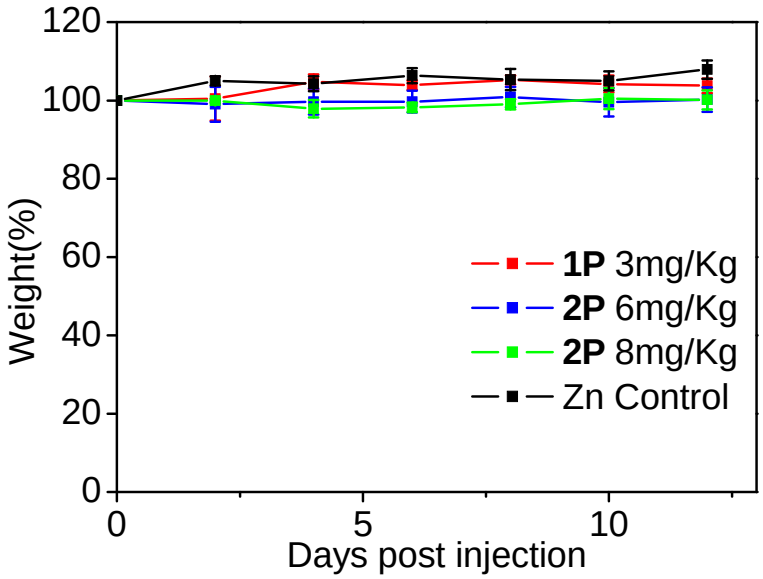

Supplementary Figure 24. Body weight of mice treated with Zn Control, **1P** and **2P** at various dose levels

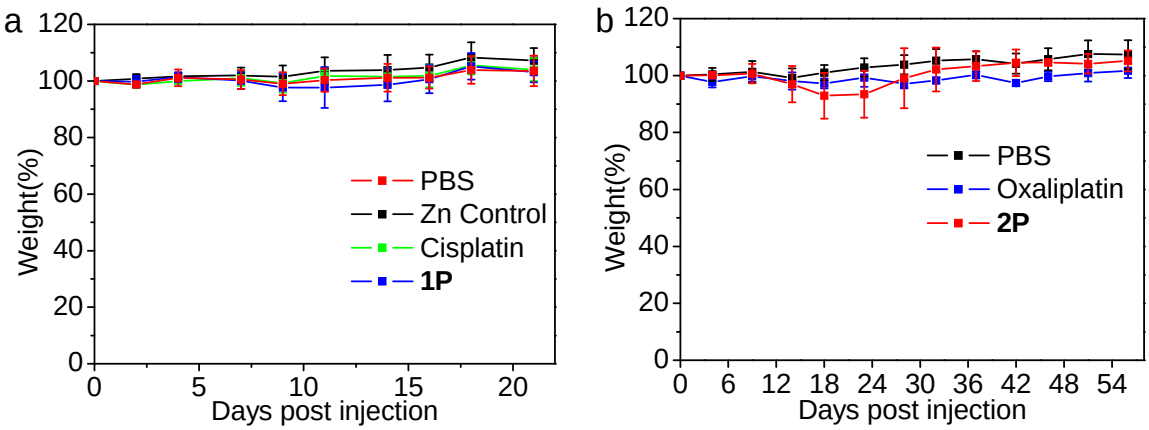

Supplementary Figure 25. Body weights of mice in different groups observed during the course of the efficacy study in H460 tumor model (a) and in AsPC-1 tumor model (b).

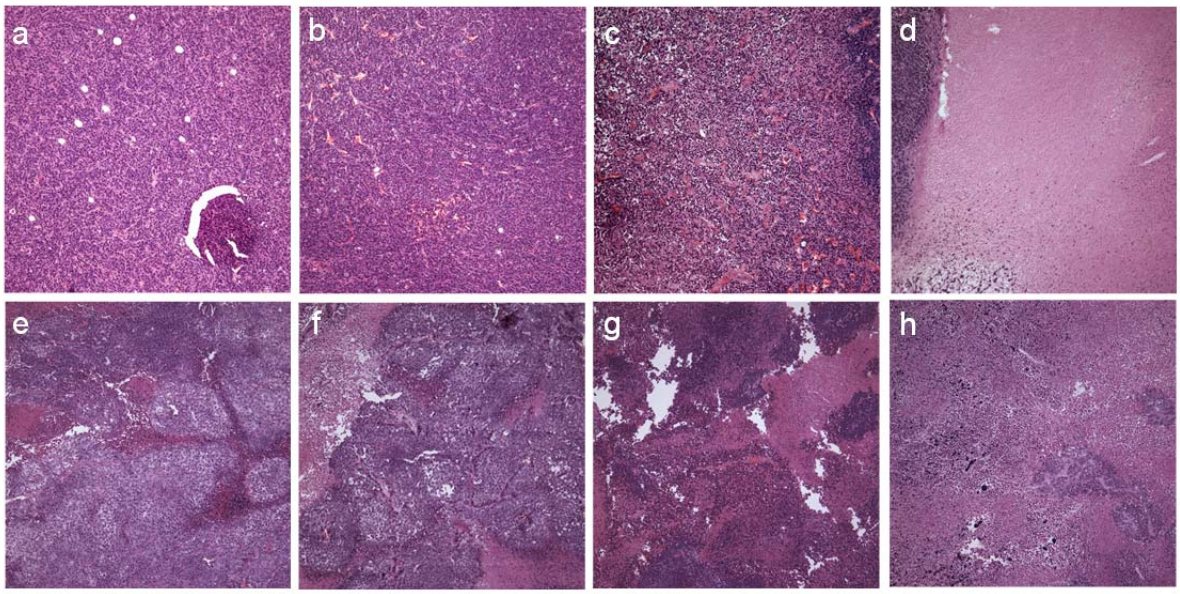

Supplementary Figure 26. Histology images of resected CT26 (a-d) and H460 (e-h) tumors (with H&E staining) from mice receiving a) and e) PBS, b) and f) Zn Control, c) and g) Cisplatin 3 mg/Kg q3d×3, d) and h) **1P** 0.5 mg/Kg q3d×3. Scale is equal to original magnification×100. The blue-purple dots are the result of nuclear staining of viable cancer cells whereas pinkish regions indicate necrotic areas of dead cancer cells.

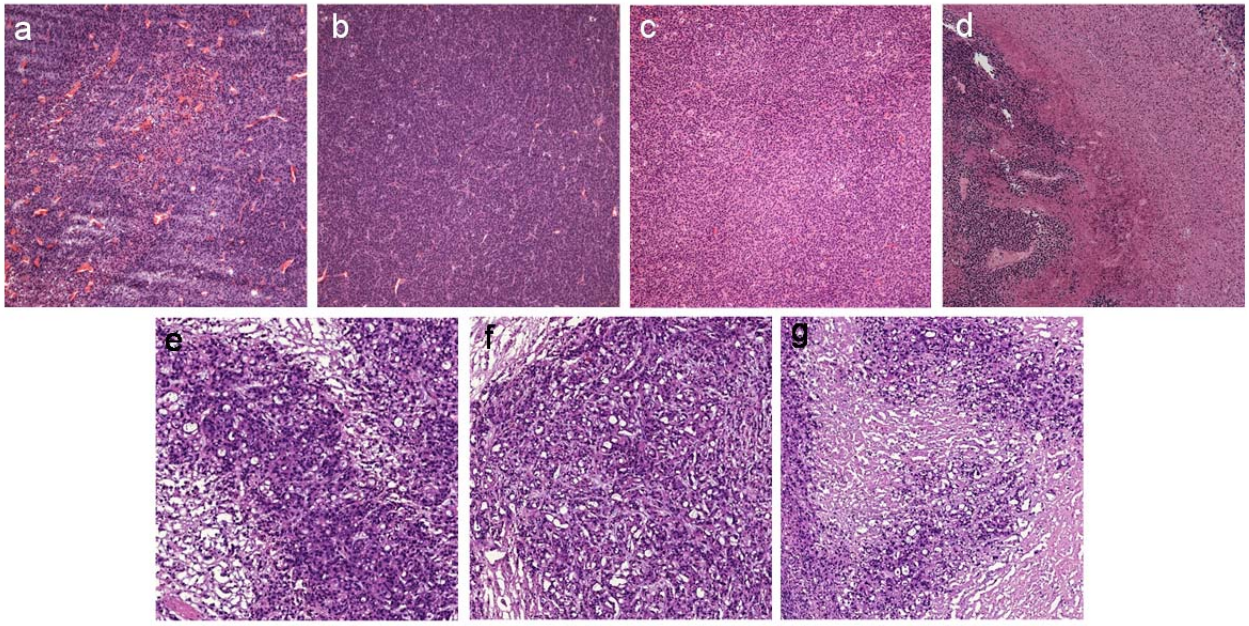

Supplementary Figure 27. Histology images of resected CT26 (a-c) and AsPC-1 (d-f) tumors (with H&E staining) from mice receiving a) PBS, b) Zn Control, c) Oxaliplatin 5 mg/Kg q2d×4, d) **2P** 2 mg/Kg q2d×4, e) PBS, f) Oxaliplatin 5 mg/Kg q4d×5, g) **2P** 2 mg/Kg q4d×5. Scale is equal to original magnification×100. The blue-purple dots are the result of nuclear staining of viable cancer cells whereas pinkish regions indicate the necrotic areas of dead cancer cells.

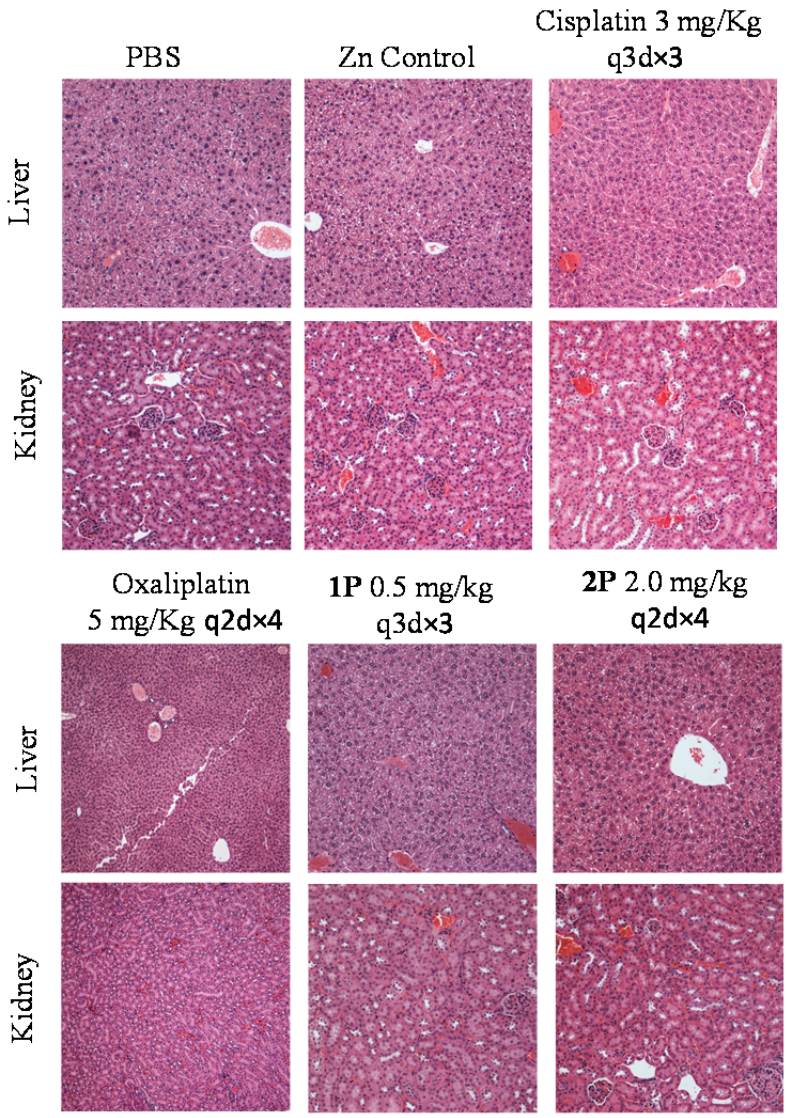

Supplementary Figure 28. Histology images of liver and kidney of CT26 tumor-bearing mice treated with various formulations. Scale is equal to original magnification×200.

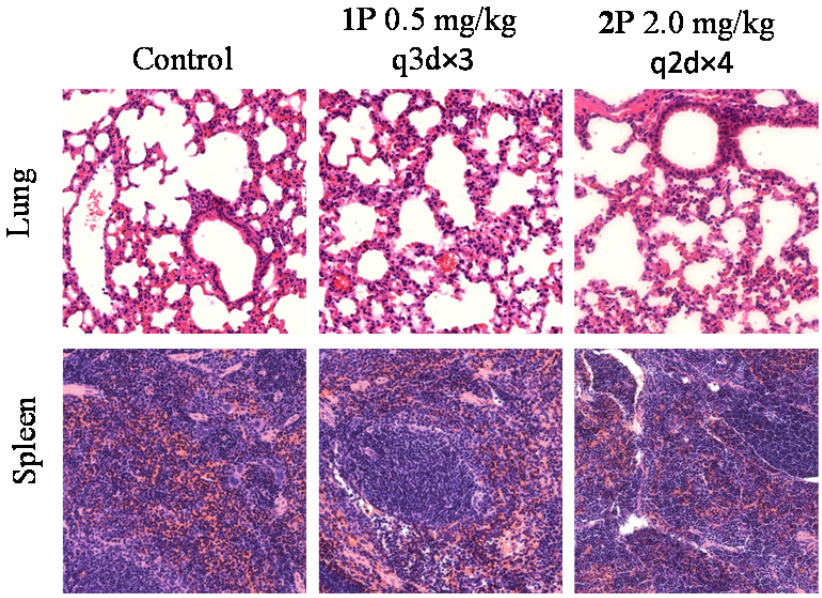

Supplementary Figure 29. Histology images of lung and spleen of CT26 tumor-bearing mice treated with various formulations. Scale is equal to original magnification×200.

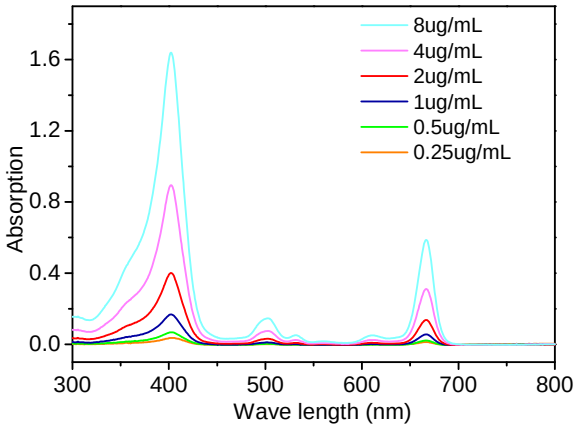

Supplementary Figure 30. UV-Vis absorption spectra of chlorin e6 in THF.

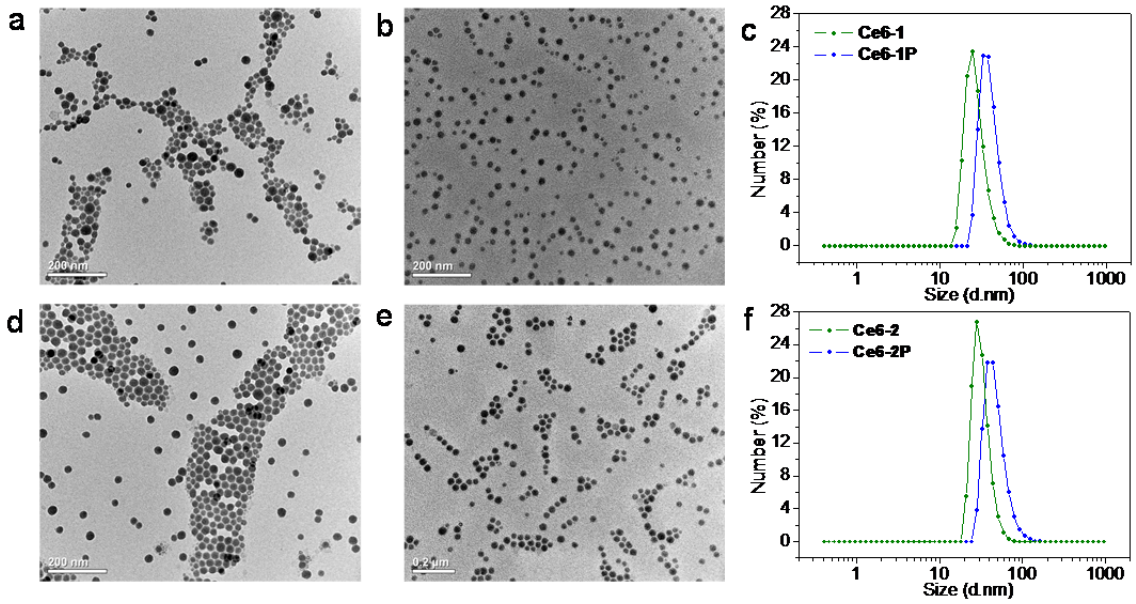

Supplementary Figure 31. TEM images of a) Ce6-**1**. b) Ce6-**1P**. d) Ce6-**2**. e) Ce6-**2P**. Size distribution of Ce6-**1** and Ce6-**1P** (c) and Ce6-**2** and Ce6-**2P** (f) measured by dynamic light scattering.

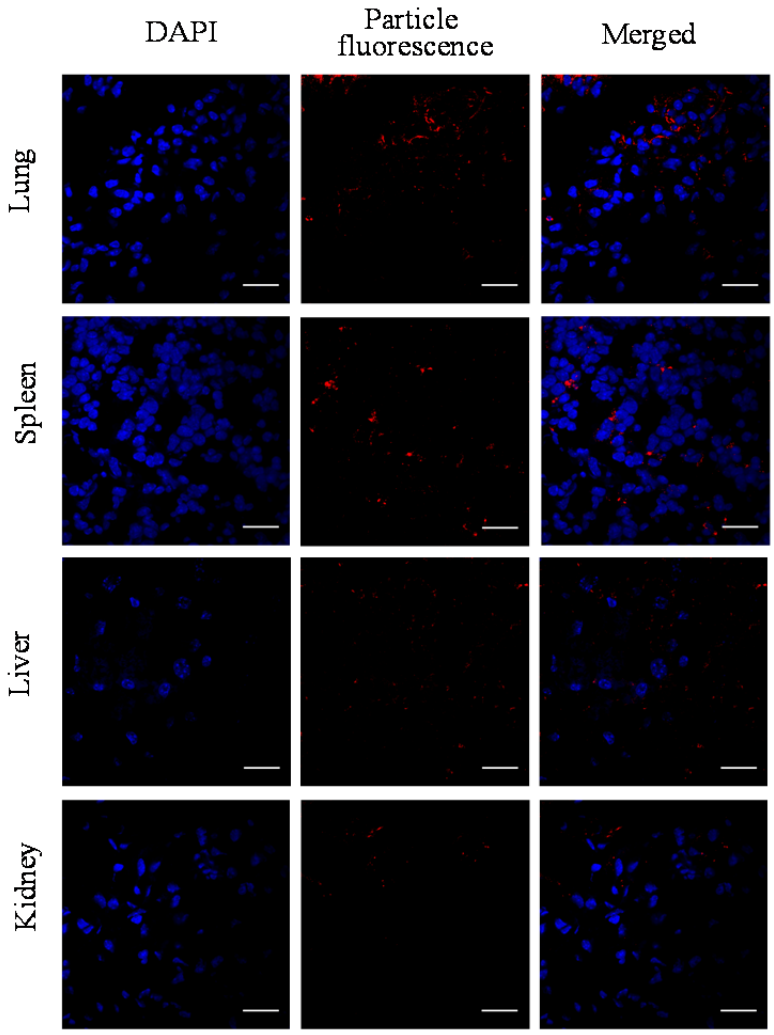

Supplementary Figure 32. Microdistributions of NCP particles in lung, spleen, liver, and kidney at 24 h post-injection. Scale bars represent 20 μm.

Supplementary Table 1. Diameter, size distribution, surface charge of DOPA-free **1** and **2**.Data are expressed as means±SD.

DOPA-free **NCPs**	TEM diameter (nm)	Number-Ave diameter (nm)	PDI*	ζ Potential (mV)
1	27.5±6.4	35.2±2.4	0.17	-10.6±2.7
2	33.6±9.7	40.4±3.2	0.06	-12.4±3.2

Supplementary Table 2. Diameter, size distribution, surface charge of Zn Control particles.

Zn Control	Number-Ave diameter (nm)	PDI	Zeta Potential (mV)
Bare	25.4±5.2[#]	0.12	NP
Pegylated	51.6±12.2[$]	0.18	-1.2±0.7

[#]Measured in THF. [$]Measured in PBS buffer. Data are expressed as means±SD.

Supplementary Table 3. Diameter, size distribution, surface charge of **1'** and **2'**.

	Number-Ave diameter (nm)	PDI	Zeta Potential (mV)
1'	39.9±2.6[#]	0.15	NP
1P'	43.3±4.2[$]	0.22	-1.2±0.4
2'	47.4±2.7[#]	0.05	NP
2P'	56.9±6.4[$]	0.17	-0.8±0.5

[#]Measured in THF. [$]Measured in PBS buffer.

Supplementary Table 4. IC_{50} values for prodrugs, cisplatin, oxaliplatin, **1P**, and **2P** in CT26, H460, and AsPC-1.

	Zn Control (μM) *	Cisplatin(μM)	Oxaliplatin(μM)	**L_1-** H4(μM)	**L_2-** H4(μM)	**1P**(μM)	**2P**(μM)
CT26	>20	5.8±0.2	7.6±0.3	6.7±0.3	10.0±0.4	9.3±0.5	10.5±0.3
H460	>20	4.0±0.2	NA	5.1±0.4	NA	5.4±0.3	NA
AsPC-1	>20	NA	10.1±0.4	NA	10.6±0.4	NA	8.8±0.6

*Zn Control does not contain cisplatin or oxaliplatin, they are served as a control to study the toxicity of excipients in NCP formulations. The amount of Zn Control particle was the same as **1P** and **2P** under the studied concentrations.

Supplementary Table 5. Pharmacokinetic parameter estimates from Zn distribution for NCPs in CT26 colon tumor bearing mice.

NCP	C_0 (μg/ml)	k_0 (1/h)	V_{ss} (mg/kg/(μg/ml))	Cl ((mg/kg)/(μg/ml)/h)	AUC (μg/ml×h)	MRT (h)	$t_{1/2}$ (h)
1P	41.8±3.9	0.023±0.002	0.06±0.006	0.001±0.0001	1808.1±151.7	43.2±5.3	30.0±4.7
2P	32.8±4.7	0.033±0.005	0.07±0.011	0.002±0.0003	987.6±128.9	30.1±5.9	20.9±3.5

Supplementary Table 6. Comparison of $AUC_{0\text{-}inf}$ and blood circulation half-lives for NCPs, prodrugs, and non-pegylated **1** in CT26 colon tumor bearing mice.

	1P	**L_1**-H_4	**2P**	**L_2**-H_4	non-pegylated **1**
$AUC_{0\text{-}inf}$	753±42.8	10.8±3.1	292±32.1	13.4±2.5	24.2±6.8
$t_{1/2}$	16.4±2.9	$t\alpha_{1/2}$= 0.02±0.003 h; $t\beta_{1/2}$= 10.2±1.7 h	12.0±3.9	$t\alpha_{1/2}$= 0.01±0.004 h; $t\beta_{1/2}$= 6.8±2.5 h	$t\alpha_{1/2}$= 0.02±0.007 h; $t\beta_{1/2}$= 77.1±12.2 h

Supplementary Table 7. Free prodrug content in blood at time point of 5 min and 60 min. Data are expressed as means±SD.

	5 min (ultrafiltrate)	5 min (plasma)	60 min (ultrafiltrate)	60 min (plasma)
1P	0.88±0.4 %ID	83.8±6.6 % ID	2.75±1.6 %ID	87.6±9.2 %ID
2P	0.43±0.2 %ID	63.1±3.4 %ID	2.23±1.0 %ID	64.4±21.2 %ID

Supplementary Table 8. Log-rank tests for free drug treated groups and NCPs treated groups.

Log Rank test	P value
1P (0.75 mg/Kg) vs. Cisplatin	0.0098
1P (0.5 mg/Kg) vs. Oxaliplatin	0.0167
2P vs. Oxaliplatin	0.0005

Supplementary Table 9. Summary of median survival time (MST) and percent increased life span (ILS (%)) of CT26 tumor bearing mice after treatment with various formulations.

Formulations	MST (days)	ILS(%)
PBS	16.3±0.8	NA
Zn Control	16.8±0.7	NA
Cisplatin (3 mg/Kg)	15.8±1.3	NA
Oxaliplatin (5 mg/Kg)	18.2±1.5	11.7
1P (0.75 mg/Kg)	22.3±1.4	36.8
1P (0.5 mg/Kg)	21.1±1.3	29.4
2P (2 mg/Kg)	29.0±1.0	77.9

Data were obtained from Fig.4 and Fig.5 and calculated with equations described in the Methods section.

Supplementary Table 10. Serum levels of BUN, CRT, AST, and ALT after chemotherapy.

Group	PBS@48h	PBS@5days	**1P**@48h	**1P**@5days	**2P**@48h	**2P**@5days	Normal Range
BUN (mg/dL)[a]	24.3±3.1	18.7±2.3	19.7±1.2	18.3±3.5	20.3±2.3	18.3±1.5	<33.7
Creatinine (mg/dL)[b]	0.17±0.06	0.1±0.0	0.17±0.06	0.1±0.0	0.27±0.06	0.2±0	<0.9
AST[c] (U/L)	140.3±22.7	174.7±20.0	189.7±26.6	153.0±43.0	158.3±26.7	169.7±36.6	<255
ALT[d] (U/L)	50.7±8.1	72.7±6.4	49.3±10.0	67.7±11.5	58±12.2	53±15.1	<132

[a]Blood urea nitrogen. [b]Creatinine. [c]Aspartate aminotransferase. [d]Alanine aminotransferase.

Supplementary Table 11. IgE levels after chemotherapy.

IgE (ng/L)	Mouse 1	Mouse 2	Mouse 3	Ave	SD	P value
Control	8.7	10.4	12.4	10.5	1.8	NA
1P	10.7	8.7	9.2	9.5	1.0	0.46
2P	6.9	14.4	18.2	13.2	5.7	0.49

Supplementary Table 12. Diameter, size distribution, surface charge of Ce6-**1** and Ce6-**2**.

	Number-Ave diameter (nm)	PDI	Zeta Potential (mV)
Ce6-**1**	27.0±1.7[#]	0.17	NP
Ce6-**1P**	39.9±6.2[$]	0.22	-1.0±0.3
Ce6-**2**	31.8±5.2[#]	0.14	NP
Ce6-**2P**	47.4±8.4[$]	0.15	-0.7±0.5

[#]Measured in THF. [$]Measured in PBS buffer.

Supplementary Table 13. Comparison of NCPs with selected formulations.

Formulation	Encapsulated drug	Carrier composition	Particle size (nm)	Drug/Prodrug loading (%)s	Blood circulation half-life in mice (h)	MTD in mice (mg/Kg)	Selected tumor models (dose based on drug)	Reference
SPI-77	Cisplatin	HSPC/Cholesterol/DSPE-PEG_{2k}	110	1.4	16	15	CT26 (6, 12, or 15mg/Kg, qwk×3), LLC (4, 7, 10, or 12 mg/Kg, qwk×3)	1
Lipoplatin	Cisplatin	HSPC/DPPG/DSPE-PEG_{2k}	110	8.9	7	5mg/kg twice per week	MCF-7 (5mg/Kg qwk), LNCaP (2.5mg/kg qwk), Panc-1 (5mg/Kg, twice per week)	2
ProLindac	Oxaliplatin prodrug	Poly(hydroxypropylmethacrylamide) based random copolymer	NA	17	23	>250	B16F10 (single i.p. dose, 200mg/Kg), M5076 (single i.p. dose, 250mg/Kg), and 2008 ovarian carcinomas (single i.p. dose, 250 mg/Kg)	3
Pt-PLGA-b-PEG-NP	Cisplatin prodrug	Poly(D,L-lactic-co-glycolic acid)-b-poly(ethylene glycol)	150	5	~4 (estimated)	>8	LNCaP (0.3 mg/Kg, biweekly for 30d)	4
CCDP/m (NC-6004)	Cisplatin prodrug	Poly(ethylene glycol)-poly(glutamic acid) block copolymer	28	39	~10(estimated)	NA	CT26 (4.0 mg/kg, q2d×5)	5
DACHPt/m (NC-4016)	Oxaliplatin prodrug	Poly(ethylene glycol)-b-poly(glutamic acid) block copolymer	40	32	~15(estimated)	NA	CT26 (4, 8, or 12 mg/kg, q2d×4), multiple metastases (8 or 12 mg/Kg, q2d×4), HT29 (8 mg/Kg, q2d×3)	6-8
1P	Cisplatin prodrug	DOPA/DOPC/Cholesterol/ DSPE-PEG_{2k}	41	48	16.4	3mg/Kg	CT26, H460(0.5 or 0.75 mg/kg q3d×3)	Current work
2P	Oxaliplatin prodrug	DOPA/DOPC/Cholesterol/ DSPE-PEG_{2k}	44	45	12.0	8mg/Kg	CT26(2.0 mg/kg, q2d×4), AsPC-1(2.0 mg/kg, q4d×5)	Current work

Supplementary Methods

Supplementary Method 1. Synthesis of bisphosphonic acid ligands based on Pt (IV) prodrugs.

Synthesis of L_1-H_4. To a suspension of *cis*, *cis*, *trans*-[$Pt(NH_3)_2Cl_2(OH)_2$](0.5 g,1.5 mmol) in 2 mL of demethylformamide (DMF) was added a 1 mL of DMF solution containing 4 equiv of the diethoxyphosphinyl isocyanate (0.92 mL, 6.0 mmol). The resulting mixture was stirred in the dark at room temperature for 12 h. The solution was filtered, and the desired product was precipitated by the addition of diethyl ether, and washed with diethyl ether for at least twice to remove the residual DMF. Yield: 80%. ^{1}H NMR in DMSO-d_6: δ 8.61 (d, 2H); 6.58 (br, 6H); 3.97 (q, 8H); 1.20 (t, 12H).

The bisphosphonate ester complex was dried under vacuum for 4 h before it was used for subsequent reactions. To a solution of the bisphosphonate ester complex (250 mg, 0.36 mmol) in 3 mL of dry DMF was added 475 uL of trimethylsilyl bromide (TMSBr, 3.6 mmol) at 0 ºC, and the mixture was allowed to react in the dark with nitrogen protection at r.t. for 18 h. After concentrating the solution, the intermediate was precipitated by the addition of dichloromethane (DCM) and further washing with DCM for at least twice. The solid was dissolved in methanol (MeOH) and stirred at room temperature for 8h in order to hydrolyze the silyl ester. After concentrating the solution, DCM was poured into the reaction mixture to precipitate the desired product, and the solid was washed with DCM twice. Yield: 60%. ^{1}H NMR in D_2O. δ 6.62 (m, 6H). ^{13}C NMR: δ 165.27 (CO_2NH). ESI-MS for $[M+H]^+$: 578.9 calcd; 579.0 found.

Synthesis of L_2-H_4. To a suspension of *cis*, *trans*-[$Pt(dach)Cl_2(OH)_2$](2.46 g, 5.94 mmol) in 12 mL of anhydrous DMF was added a 10 mL DMF solution containing 4 equiv of the diethoxyphosphinyl isocyanate (3.7 mL, 24 mmol). The resulting mixture was stirred in the dark at r.t. for12 h. The solution was filtered, and the bisphosphonate ester product was precipitated by the addition of diethyl ether, and washed with diethyl ether for at least twice to remove the residual DMF. Yield: 62%. ^{1}H NMR in DMSO-d_6: δ 9.36 (br, 2H); 8.72 (d, 2H); 8.15 (br, 2H); 4.38 (m, 8H); 2.72 (t, 2H); 2.26 (d, 2H); 1.56 (d, 2H); 1.35 (m, 2H); 1.07 (m, 2H).

The bisphosphonate ester complex was dried under vacuum for 4 h before it was used for subsequent reactions. To a solution of the ester complex (2.85 g, 3.69 mmol) in 5.5 mL of anhydrous DMF was added 5.0 mL of trimethylsilyl bromide (38 mmol) at 0 ^{o}C. The mixture was allowed to react in the dark with nitrogen protection at r.t. for 18 h. After concentrating the solution, the intermediate was precipitated by the addition of dichloromethane and further washing with DCM for at least twice. The solid was dissolved in MeOH and stirred at room temperature for 8h in order to hydrolyze the silyl ester. After concentrating the solution, DCM was poured into the reaction mixture to precipitate the desired product, and the solid was washed with DCM twice. Yield: 94 %. ^{1}H NMR in D_2O: δ2.94 (m, 2H); 2.26 (d, 2H);

1.55 (m, 4H); 1.22 (m, 2H). ^{13}C NMR: δ 166.65 (CO_2NH), δ 62.93 (CNH_2), δ 31.30 and δ 23.33 (CH_2CH_2). ESI-MS for $[M+H]^+$: 659.0 calcd; 659.0 found.

Supplementary Method 2. Determination of NCP Formulae by ICP-MS and TGA.

The formula of 1. Pre-weighted dry nanoparticles were digested in concentrated nitric acid overnight and then diluted with water for ICP-MS analysis. The prodrug loading in **1** without DOPA coating was determined to be 68.2 wt.% and the Zn content was determined to be 22.2 wt.%. Thus the molar ratio of Pt:Zn was determined to be 1:3. The solvent weight loss determined by TGA is about 8 wt.%. The complete formula thus was established to be $Zn_3 \cdot \mathbf{L_1} \cdot (OH)_2 \cdot 4H_2O$. The expected weight remained based on this formula is 66.1 wt.% which matches with the observed weight remained by TGA (66.7 wt.%). The prodrug loading in **1** with DOPA coating was determined to be 48.0 wt.% and the Zn content was determined to be 20.4 wt.%. Thus the molar ratio of Pt:Zn was determined to be 1:3.5. The solvent weight loss determined by TGA is about 5 wt.%. The complete formula thus was established to be $Zn_{3.5} \cdot \mathbf{L_1} \cdot DOPA_{0.3} \cdot (OH)_{2.7} \cdot 3H_2O$. The expected weight remained based on this formula is 58 wt.%. The observed weight remained by TGA is 62 wt.%.

The formula of 2. Pre-weighted dry nanoparticles were digested in concentrated nitric acid overnight and then diluted with water for ICP-MS analysis. The prodrug loading in **2** without DOPA coating was determined to be 63.5 wt.% and the Zn content was determined to be 20.1 wt.%. Thus the molar ratio of Pt:Zn was determined to be 1:3. The solvent weight loss determined by TGA is about 7 wt.%. The complete formula thus was established to be $Zn_3 \cdot \mathbf{L_2} \cdot (OH)_2 \cdot 4H_2O$. The expected weight remained based on this formula is 60.6 wt.% which matches with the observed weight remained by TGA (61.8 wt.%). The prodrug loading in **2** (with DOPA coating) was determined to be 49.2 wt.% and the Zn content was determined to be 17.5 wt.%. Thus the molar ratio of Pt:Zn was determined to be 1:3.5. The solvent weight loss determined by TGA is about 7 wt.%. The complete formula thus was established to be $Zn_{3.5} \cdot \mathbf{L_2} \cdot DOPA_{0.3} \cdot (OH)_{2.7} \cdot 5H_2O$. The expected weight remained based on this formula is 52.1 wt.%. The observed weight remained by TGA is 56.4 wt.%.

The formulae of 1P and 2P. Pre-weighted dry nanoparticles of **1P** and **2P** were digested in concentrated nitric acid overnight and then diluted with water for ICP-MS analysis. The prodrug loading in **1P** and **2P** were determined to be 41±4 wt.% and 38±6 wt.%, respectively. By comparing these numbers with the drug loading values for **1** and **2**, the total lipid and lipid-peg amount was calculated to be around 18 wt% for both **1P** and **2P**. The molar ratio for DOPC, cholesterol, and DSPE-PEG_{2k} is 0.4:0.4:0.2. The average molecular weight for this lipid composition is 1030 g/mol. The final formula of **1P** was determined to be

0.24[0.4(DOPC):0.4(Chol):0.2(DSPE-PEG_{2k})]·$Zn_{3.5}$·$\mathbf{L_1}$·$(DOPA)_{0.3}$·$(OH)_{2.7}$·$3H_2O$, and the final formula of **2P** was determined to be 0.26[0.4(DOPC):0.4(Chol):0.2(DSPE-PEG_{2k})]·$Zn_{3.5}$·$\mathbf{L_2}$·$(DOPA)_{0.3}$·$(OH)_{2.7}$·$5H_2O$.

Supplementary Method 3. Synthesis of Zn Control particles.

Microemulsions were first formed by the addition of 25mg/mL $Na_4P_2O_7·10H_2O$ and 100 mg/mL $Zn(NO_3)_2·6H_2O$ to two separate TritonX-100 (100 mL, 0.3 M, 1.5 M cyclohexane/hexanol) surfactant system mixtures. The separate microemulsions were stirred vigorously for 10 to 15 min at room temperate, after which they were combined, and the resultant microemulsion was allowed to stir vigorously for 30 min at room temperature. After the adding of 20 mL ethanol, particles were washed once with ethanol and twice with 50% EtOH/THF, and redispersed in THF.

Supplementary Method 4. Quantification of Triton X-100 Amount in NCPs.

The amounts of Triton X-100 in NCP formulations were quantified by following the reported procedures.[9] The standard curve was constructed using the following concentrations: 1, 5, 10, 50, and 100 μg/ml. NCP particles (18 mg) were digested in 12 M NaOH at 70 ^oC. Cyclohexane was used to extract Triton X-100 from aqueous phase. After rotary evaporation, samples were dissolved in acetonitrile (2 mL) and analyzed by HPLC. HPLC (LC-10AT VP, Shimadzu, Japan) equipped with SPD-M10A VP diode array detector, SIL-10AF auto injector and SCL-10A VP system controller. Column: Dynamax-300A C18 (250×4.14 mm, 5 μm) (Rainin Instrument Co. InC., Woburn, MA); mobile phase: acetonitrile: water=50:50 (v/v); flow rate: 1.0 mL/min; wavelength: 200 nm.
Our detection limit for Triton X-100 is about 1 ug/ mL. The highest possible Triton X-100 amount in the NCP particles is 0.11 μg per mg of NCP. By applying those washing steps, Triton X-100 was nearly completely removed.

Supplementary Method 5. ^{195}Platinum NMR investigation of the reduction reaction of Pt (IV) prodrugs.

^{195}Pt NMR spectra were referenced externally using standards of K_2PtCl_4 in D_2O (δ=-1628 ppm). The reduction of $\mathbf{L_1}$-H_4 and $\mathbf{L_2}$-H_4 was performed in aqueous solution by treatment with 1 equiv of cysteine. Water was removed in vacuo. The observed chemical shift matches with reported Pt (IV) complexes with similar structures and the three peaks observed for $\mathbf{L_1}$-H_4 and $\mathbf{L_2}$-H_4 is due to possible conformational isomers.[10] The complexes formed after the treatment of cysteine with chemical shifts around -2000 ppm are assigned to Pt(II) complexes.[11]

Supplementary Method 6. Particle stability and release profiles.

Dynamic light scattering measurements of **1P** and **2P** in PBS buffer were carried out in the presence of bovine serum albumin at a concentration of over 5 mg/mL at 37 ^{o}C. Particle size, PDI, and count rate were recorded over a 16 - 20 h period.

Dynamic light scattering measurements of **1P** and **2P** in PBS supplemented with 10% fetal bovine serum (FBS) at 37^{o}C. Particle size, PDI, count rate, and ζ potential were recorded over a 24 h period.

The release profiles were performed in 400 mL of 5 mM PBS buffer at 37 ^{o}C. The NCPs (3 mg) were suspended in 5 mL 5 mM PBS buffer in a 10,000 MWCO pleated dialysis bag. The dialysis bag containing nanoparticle suspension was then put in the beaker followed by the addition of 400 mL of 5 mM PBS buffer, and the system was incubated at 37 ºC under stirring . Periodically, 1 mL aliquots of the solution were removed, and 1 mL of fresh buffer solution was added to the beaker. The removed aliquots were collected and analyzed by ICP-MS for Pt and Zn contents. For reducing experiment, 5mM cysteine was used for the release profiles.

The release profiles were also performed in 400 mL of cell culture medium with 10% FBS at 37 ^{o}C. The NCPs (3 mg) were suspended in 5 mL cell culture medium with 10% FBS in a 10,000 MWCO pleated dialysis bag. The dialysis bag containing nanoparticle suspension was then put in the beaker followed by the addition of 400 mL of RPMI-1640 medium with 10% FBS, and the system was incubated at 37 ºC under stirring . Periodically, 1 mL aliquots of the solution were removed, and 1 mL of fresh buffer solution was added to the beaker. The removed aliquots were collected and analyzed by ICP-MS for Pt and Zn contents. For reducing experiment, 5mM cysteine was used for the release profiles.

Supplementary Method 7. Synthesis of Rhodamine B-doped NCP.

A w=7.4 microemulsion was prepared by the addition of 0.2 mL of a 25mg/mL $\mathbf{L_1}$-Na_4 aqueous solution, 20uL of rhodamine B sodium salt solution and 0.22 mL of a 100mg/mL $Zn(NO_3)_2$ aqueous solution to separate 5.5 mL aliquots of a 0.3 M Triton X-100/1.5 M 1-hexanol in cyclohexane mixture while vigorously stirring at room temperature. 20 uL DOPA (200mg/mL in $CHCl_3$) was added to the complex solution and the stirring was continued for 15mins until clear solution formed. The two microemulsions were combined, and the resultant 11 mL microemulsion with w=7.4 was stirred for an additional 30 minutes. After the adding of 20 mL ethanol, **1'** were washed once with ethanol and twice with 50%

EtOH/THF, and redispersed in THF. The cisplatin prodrug loading was determined to be 57.3 wt.% by ICP-MS and rhodamine B loading was quantified by UV-Vis spectroscopy to be 0.5 wt.%. **2'** was synthesized via the same condition. The oxaliplatin prodrug loading was determined to be 53.4 wt.% by ICP-MS and rhodamine B loading was quantified by UV-Vis spectroscopy to be 0.8 wt.%.

Supplementary Method 8. Visualization of the Apoptosis of Cancer Cells Induced by NCPs.

Coverslips putting in the 6-well plates were seeded with CT26 cells at the density of 1×106 cells per well. The cells were incubated at 37°C and 5% CO_2 for 24 h prior to nanoparticle treatment. **1P** and **2P** doped with Rhodamine B were incubated with cells at drug concentration of 10 μM at 37°C and 5% CO_2 for 24 h. Then, the cells were washed with PBS, fixed with iced 4% paraformaldehyde. The apoptosis was detected by TUNEL reaction using DNA fragmentation detection kit (Life Technology, USA). The nuclei were stained with 10 ug/mL of 4',6-diamidino-2-phenylindole (DAPI). The cells were observed using Olympus Fluoview 1000 confocal laser scanning microscope (CLSM) at excitation wavelength of 405 nm, 488 nm, and 543 nm to visualize nuclei (blue), cell apoptosis (green fluorescence), and NCPs (red fluorescence), respectively.

Supplementary Method 9. DNA ladder experiments.

CT26 cells were seeded at 1×10^6 cells per well in 6-well plates and further cultured for 24 h. The culture media were replaced by 2 mL of fresh culture media containing 10% FCS. **1P**, cisplatin, cisplatin prodrug (**L_1**-H_4), **2P**, oxaliplatin, and oxaliplatin prodrug (**L_2**-H_4) were added to the cells at drug concentrations of 10 μM. Zn control nanoparticles served as control. Following incubation for 24 h, total DNA of cancer cells was extracted using DNA ladder isolation kit (Sigma-Aldrich, USA) according to the manufacture instructions and examined for DNA fragmentation on a 2% (w/v) agarose gel electrophoresis at 35 V for 3 h.

Supplementary Method 10. *In vitro* cytotoxicity assays.

The cytotoxicity of cisplatin, **L_1**-H_4, and **1P** was evaluated in CT26 and H460 cells, while the cytotoxicity of oxaliplatin, **L_2**-H_4, and **2P** was evaluated in CT26 and AsPc-1 cells. The cytotoxicity of Zn Control was also determined in CT26, H460, and AsPc-1 cells.

CT26, H460, and AsPc-1 cells were seeded at 2000 cells per well in 96-well plates and further cultured for 24 h. The culture media were replaced by 100 μL of fresh culture media containing 10% FBS. Cisplatin, $\mathbf{L_1}$-H_4, **1P**, oxaliplatin, $\mathbf{L_2}$-H_4, **2P**, and Zn Control were added to the cells at different cisplatin or oxaliplatin doses. Following incubation for 48 h, the cell viability was determined by (3-(4,5-dimethylthiazol-2-yl)-5-(3-carboxymethoxyphenyl)-2-(4-sulfophenyl)-2H-tetrazolium) (MTS) assay (Promega, USA) according to manufacturer's instructions. The concentrations of cisplatin or oxalipaltin required to inhibit cell growth by 50% (IC_{50} values) were calculated.

Supplementary Method 11. Internalization mechanism of NCPs.

To explore the mechanism involved in the uptake process, CT26 cells were pre-incubated with uptake inhibitors including chlorpromazine (10 μg/mL, clathrin-mediated endocytosis inhibitor), genistein (200 μg/mL, caveolae-mediated endocytosis inhibitor), methyl-β-cyclodextrin (Me-β-CD, 50 μM, lipid-raft-mediated endocytosis inhibitor), wortmannin (50 nM, macropinocytosis inhibitor), and NaN_3 (10 mM, energy-dependent endocytosis inhibitor) for 30 min prior to nanoparticle application and throughout the 4-h uptake experiment at 37 °C. The Pt uptake amount was determined by ICP-MS. Results were expressed as percentage uptake of the control where cells were incubated with **1P** at 37 °C for 4 h.

To visualize co-localization of internalized **1P** with endosomal/lysosomal compartments, CT 26 cells were incubated with **1P'** for 2 h at 37 °C. Then, cells were stained with DAPI (10 μg/mL) and Lysotracker Green (100 nM) before observation with CLSM.

To explore caveolae-mediated endocytosis, **1P'** and Chlorea Toxin Subunit B (CT-B) Alexa Fluor488 (5 μg/mL) of which the internalization pathway was demonstrated to be caveolae-dependent were simultaneously incubated with CT26 cells for 2 h at 37 °C. The cells were stained with DAPI (10 μg/mL) and observed for intracellular fluorescence distribution using CLSM.

Supplementary Method 12. Ultrafiltration experiment.

Mice were injected with **1P** and **2P** at dose of 3 mg/Kg cisplatin or oxaliplatin. At time point of 5 min and 60 min, blood was withdrawn and centrifuged for 10 min at 3000 rpm to obtain the plasma. Ultra-filtrated plasma samples were obtained by centrifuging the plasma fraction through a 10-KDa cut-off ultrafiltration filter for 15min at 13000 rpm. ICP-MS was used to determine Pt content in ultrafiltrate plasma.

Supplementary Method 13. Determination of maximum tolerated dose for **1P** and **2P**.

The maximum tolerated doses (MTD) of **1P** and **2P** after a single i.v. injection to female Balb/c mice were examined. The MTD was determined based on the group that all mice survived and did not lose over 20% weight. The MTD of **1**P and **2**P were 3 mg/Kg and 8 mg/Kg, respectively.

Supplementary Method 14. Immunoglobulin E (IgE) measurements.

CT26 tumor bearing mice were intravenously injected with **1P** (0.75 mg/Kg, q3d×3), **2P** (2.0 mg/Kg, q2d×4), and saline (control). Twenty-four hours after the last injection, the blood of the mice was withdrawn followed by the separation of the serum. IgE concentrations in serum were determined by mouse IgE ELISA kit (Abcam, Cambridge, MA) according to the manufacturer's instructions. No elevated IgE levels were observed after NCP administrations.

Supplementary Method 15. Synthesis of chlorin e6-doped NCP.

A w=7.4 microemulsion was prepared by the addition of 0.2 mL of a 25mg/mL $\mathbf{L_1}$-Na_4 aqueous solution, 20uL of chlorin e6 sodium salt solution and 0.22 mL of a 100mg/mL $Zn(NO_3)_2$ aqueous solution to separate 5.5 mL aliquots of a 0.3 M Triton X-100/1.5 M 1-hexanol in cyclohexane mixture while vigorously stirring at room temperature. 20 uL DOPA (200mg/mL in $CHCl_3$) was added to the complex solution and the stirring was continued for 15mins until clear solution formed. The two microemulsions were combined, and the resultant 11 mL microemulsion with w=7.4 was stirred for an additional 30 minutes. After the adding of 20 mL ethanol, Ce6-**1** were washed once with ethanol and twice with 50% EtOH/THF, and redispersed in THF. The cisplatin prodrug loading was determined to be 46.4 wt.% by ICP-MS and chlorin e6 loading was quantified by UV-Vis spectroscopy to be 1.2 wt.%. Ce6-**2** was synthesized via the same condition. The oxaliplatin prodrug loading was determined to be 43.6 wt.% by ICP-MS and chlorin e6 loading was quantified by UV-Vis spectroscopy to be 1.7 wt.%.

Supplementary Discussion 1. Pharmocokinetic study and biodistribution assessed by Zn.

Although we present the pK and biodistribution data assessed by Zn here, due to different Zn concentrations in different organs (we subtracted the background Zn by evaluating several control mice without particle treatment), we don't think the distribution of Zn determined here will be a good

representative of nanoparticle distribution in vivo. However, since the background Zn concentration is much lower in blood than in major organs, the circulation profiles in blood still follow the same trend as assessed by Pt.

Supplementary References

1. Newman, M.S., Colbern, G.T., Working, P.K., Engbers, C. & Amantea, M.A. Comparative pharmacokinetics, tissue distribution, and therapeutic effectiveness of cisplatin encapsulated in long-circulating, pegylated liposomes (SPI-077) in tumor-bearing mice. *Cancer Chemother. Pharmacol.* **43**, 1-7 (1999).
2. Boulikas, T. Low toxicity and anticancer activity of a novel liposomal cisplatin (Lipoplatin) in mouse xenografts. *Oncol. Rep.* **12**, 3 (2004).
3. Rice, J.R., Gerberich, J.L., Nowotnik, D.P. & Howell, S.B. Preclinical Efficacy and Pharmacokinetics of AP5346, A Novel Diaminocyclohexane-Platinum Tumor-Targeting Drug Delivery System. *Clin. Cancer Res.* **12**, 2248-2254 (2006).
4. Dhar, S., Kolishetti, N., Lippard, S.J. & Farokhzad, O.C. Targeted delivery of a cisplatin prodrug for safer and more effective prostate cancer therapy in vivo. *Proc. Natl. Acad. Sci.* **108**, 1850-1855 (2011).
5. Nishiyama, N. et al. Novel Cisplatin-Incorporated Polymeric Micelles Can Eradicate Solid Tumors in Mice. *Cancer Res.* **63**, 8977-8983 (2003).
6. Cabral, H., Nishiyama, N., Okazaki, S., Koyama, H. & Kataoka, K. Preparation and biological properties of dichloro(1,2-diaminocyclohexane)platinum(II) (DACHPt)-loaded polymeric micelles. *J. Controlled Release* **101**, 223-232 (2005).
7. Cabral, H., Nishiyama, N. & Kataoka, K. Optimization of (1,2-diamino-cyclohexane)platinum(II)-loaded polymeric micelles directed to improved tumor targeting and enhanced antitumor activity. *J. Controlled Release* **121**, 146-155 (2007).
8. Murakami, M. et al. Improving Drug Potency and Efficacy by Nanocarrier-Mediated Subcellular Targeting. *Sci. Transl. Med.* **3**, 64ra62 (2011).
9. Heinig, K. & Vogt, C. Determination of Triton X-100 in influenza vaccine by high-performance liquid chromatography and capillary electrophoresis. *Fresenius J. Anal. Chem.* **359**, 202-206 (1997).
10. Wilson, J.J. & Lippard, S.J. Synthesis, Characterization, and Cytotoxicity of Platinum(IV) Carbamate Complexes. *Inorg. Chem.* **50**, 3103-3115 (2011).
11. Truflandier, L.A., Sutter, K. & Autschbach, J. Solvent Effects and Dynamic Averaging of 195Pt NMR Shielding in Cisplatin Derivatives. *Inorg. Chem.* **50**, 1723-1732 (2011).